Visible Light Communication, Networking, and Sensing: A Survey, Potential and Challenges

Parth H. Pathak, Xiaotao Feng, Pengfei Hu, and Prasant Mohapatra

***Abstract*—The solid-state lighting is revolutionizing the indoor illumination. Current incandescent and fluorescent lamps are being replaced by the LEDs at a rapid pace. Apart from extremely high energy efficiency, the LEDs have other advantages such as longer lifespan, lower heat generation, and improved color rendering without using harmful chemicals. One additional benefit of LEDs is that they are capable of switching to different light intensity at a very fast rate. This functionality has given rise to a novel communication technology (known as visible light communication—VLC) where LED luminaires can be used for high speed data transfer. This survey provides a technology overview and review of existing literature of visible light communication and sensing. This paper provides a detailed survey of 1) visible light communication system and characteristics of its various components such as transmitter and receiver; 2) physical layer properties of visible light communication channel, modulation methods, and MIMO techniques; 3) medium access techniques; 4) system design and programmable platforms; and 5) visible light sensing and application such as indoor localization, gesture recognition, screen-camera communication, and vehicular networking. We also outline important challenges that need to be addressed in order to design high-speed mobile networks using visible light communication.**

***Index Terms*—Visible light communication, LEDs, solid-state lighting, mobile communication, smart lighting, mobile computing, visible light sensing, wireless networks, localization and sensing, screen-camera links.**

I. Introduction

THE in door lighting is going through a revolution. The incandescent bulb that has been widely used to lit our surroundings since its invention over a century ago is slowly being phased out due to its extremely low energy efficiency. Even in the most modern incandescent bulbs, no more than 10% of the electrical power is converted to useful emitted light. The compact fluorescent bulbs introduced in 1990s have gained increasing popularity in the last decade as they provide a better energy efficiency (more lumens per watt). However, recent advancements in solid-state lighting through Light Emitting Diodes (LEDs) have enabled unprecedented energy efficiency and luminaire lifespan. Average luminous efficacy (how much electricity is used to provide the intended illumination) of best-in-class LEDs is as high as 113 lumens/watt in 2015 [1], and is projected to be around 200 lumens/watt by the year 2020. This is a many fold increase compared to current incandescent and fluorescent bulbs which provide an average luminous efficacy of 15 and 60 lumens/watt [1] respectively. Similarly, the lifespan of LEDs ranges from 25 000 to 50 000 hours significantly higher than compact fluorescent (10 000 hours). Apart from the energy savings and lifespan advantages, the LEDs also have other benefits like compact form factor, reduced usage of harmful materials in design and lower heat generation even after long period of continuous usage. Due to these benefits, LED adoption is on a consistent rise and it is expected that nearly 75% of all illumination will be provided by LEDs by the year 2030 [1].

The rapid increase in the usage of LEDs has provided a unique opportunity. Different from the older illumination technologies, the LEDs are capable of switching to different light intensity levels at a very fast rate. The switching rate is fast enough to be imperceptible by a human eye. This functionality can be used for communication where the data is encoded in the emitting light in various ways. A photodetector (also referred as a light sensor or a photodiode) or an image sensor (matrix of photodiodes) can receive the modulated signals and decode the data. This means that the LEDs can serve dual purpose of providing illumination as well as communication. In last couple of years, VLC research has shown that it is capable of achieving very high data rates (nearly 100 Mbps in IEEE 802.15.7 standard and upto multiple Gbps in research). The communication through visible light holds special importance when compared to existing forms of wireless communications. First, with the exponential increase of mobile data traffic in last two decades has identified the limitations of RF-only mobile communications. Even with efficient frequency and spatial reuse, the current RF spectrum is proving to be scarce to meet the ever-increasing traffic demand. Compared to this, the visible light spectrum which includes hundreds of terahertz of license free bandwidth (see Fig. 1) is completely untapped for communication. The Visible Light Communication (VLC) can complement the RF-based mobile communication systems in designing high-capacity mobile data networks. Second, due to its high frequency, visible light cannot penetrate through most objects and walls. This characteristic allows one to create small cells of LED transmitters with no inter-cell interference issues beyond the walls and partitions. It can also increase the capacity of available wireless channel dramatically. The inability of signals to penetrate through the walls also provides an inherent wireless communication security. Third, VLC facilitates the reuse of existing lighting infrastructure for the purpose of communication. This means that such systems can be deployed with relatively lesser efforts and at a lower cost. This untapped potential of

Manuscript received February 2, 2015; revised July 14, 2015; accepted August 27, 2015. Date of publication September 3, 2015; date of current version November 18, 2015.

P. H. Pathak, P. Hu, and P. Mohapatra are with the Department of Computer Science, University of California, Davis, CA 95616-8562 USA (e-mail: phpathak@ucdavis.edu; pfhu@ucdavis.edu; pmohapatra@ucdavis.edu).

X. Feng is with the Department of Electrical and Computer Engineering, University of California, Davis, CA 95616 USA (e-mail: xtfeng@ucdavis.edu).

Digital Object Identifier 10.1109/COMST.2015.2476474

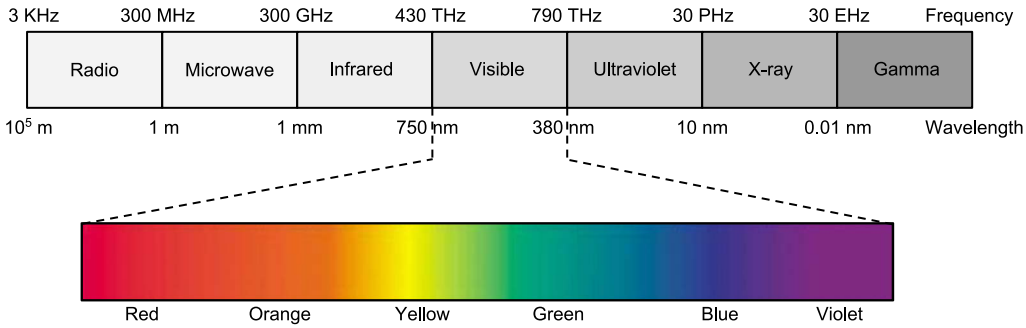

Fig. 1. Human eye can perceive the electromagnetic signals between the frequency range of 430 THz and 790 THz which is referred as the visible light spectrum.

visible light communication has motivated us to compile this survey.

The pioneering efforts of utilizing LEDs for illumination as well as communication date back to year 2000 when researchers [2] in Keio University in Japan proposed the use of white LED in homes for building an access network. This was further fueled by rapid research, especially in Japan, to build high-speed communication through visible light with development of VLC support for hand-held devices and transport vehicles. This led to formation of Visible Light Communications Consortium (VLCC) [3] in Japan in November of 2003. VLCC proposed two standards—Visible Light Communication System Standard and Visible Light ID System Standard—by 2007. These standards were later accepted by Japan Electronics and Information Technology Industries Association (JEITA) [4] as JEITA CP-1221 and CP-1222 respectively. The VLCC also incorporated and adapted the infrared communication physical layer proposed by international Infrared Data Association (IrDA) [5] in 2009. In parallel, hOME Gigabit Access project (OMEGA) [6], sponsored by European Union, also developed optical communication as a way to augment the RF communication networks. In 2014, VLCA (Visible Light Communications Associations) [7] is established as a successor of VLCC in Japan for further standardization of VLC. The first IEEE standard for visible light communication was proposed in 2011 in the form of IEEE 802.15.7 [8] which included the link layer and physical layer design specifications. In last couple of years, the achievable VLC link capacity has surpassed 1 Gbps, and increasing research efforts are being directed towards realizing the full potential of VLC.

In this survey, we provide a systematic view of VLC research and identify important challenges. Specifically, we provide technology overview and literature review of

1) Visible light communication system components and, details of transmitter and receiver characteristics,
2) Physical layer characteristics such as channel model and propagation, modulation and coding schemes, and Multiple-Input Multiple-Output (MIMO) techniques,
3) Link layer, multiple user access techniques and issues,
4) System design and various programmable VLC platforms,
5) Visible light sensing and applications such as visible light indoor localization, human computer interaction, device-to-device communication and vehicular communication applications.

Based on the review, we then outline a list of challenges that need to be addressed in future research to realize full potential of VLC.

The growing interest in VLC has resulted in a few surveys in past couple of years. This article differs from these surveys in many ways. In [9], authors discussed LED-based VLC where the primary focus of discussion was on design of physical layer techniques (modulation, circuit design etc.) that can enhance the performance of VLC. Compared to [9], this article focuses on a broader discussion about VLC, covering other aspects of networking such as medium access as well as sensing using visible light. Medium access protocols for VLC have been surveyed in [10], however, no comprehensive overview and comparison of networking techniques have been provided. Also, in this paper, we show that the usage of smartphone camera and light sensor for receiving visible light signals extend the VLC to other related fields of mobile computing and sensing. Multiple research topics in this area such as indoor localization and smartphone screen-camera communication are not surveyed in any earlier work before this paper. In this paper, we provide a comprehensive survey of these topics with additional focus on *visible light sensing*. Compared to [11] and [12] where authors surveyed free-space communication along with other forms of optical wireless communications, the primary focus of this survey is narrower and more detailed towards visible light communication. In another related survey, authors provided a detailed overview of how optical wireless communication can be used for cellular network design in [13], with different aspects of outdoor environment and its impact on the communication performance. Compared to this, our primary focus in this paper is on visible light communication primarily in indoor settings. Authors provided a brief survey of VLC applications in [14] with some discussion on vehicular networks and indoor broadcasting. However, in this paper, we survey a growing body of literature since the publication of [14] focusing on novel applications of VLC such as indoor localization, screen-camera communication etc. We also detail various practical aspects of communication system design by reviewing currently available programmable platforms and LED transmitters/receivers. This will enable researchers with RF communication background to easily extend their expertise in visible light wireless access networks.

The rest of the survey is organized as follows. We start by providing an overview of various components of a visible light communication system with introduction to LED luminaires and different types of receivers in Section II. In Section III,

we survey the physical layer properties of VLC with details on channel and propagation, modulation methods and MIMO techniques. It also includes an overview of VLC standard IEEE 802.15.7 [8]. This is followed by Section IV where various link layer and medium access protocols are discussed. Section V describes various aspects of VLC system design and surveys available programmable platforms that can be used for research. Section VI reviews a wide variety of topics in visible light sensing and applications which includes indoor localization, screen-camera communication, vehicular communication and human-computer interaction. Based on the review, Section VII outlines various challenges that need further research in order to build high-capacity, mobile VLC networks. We have compiled the acronyms used throughout the paper and presented them with their full forms in Table I.

II. VLC System Overview

In this section, we provide an overview of visible light communication system and its transmitter and receiver components. We then discuss various modes of VLC.

A. VLC Transmitter

The transmitter in a visible light communication system is an LED luminaire. An LED luminaire is a complete lighting unit which consists of an LED lamp, ballast, housing and other components. The LED lamp (also referred as an LED bulb in simpler terms) can include one or more LEDs. The lamp also includes a driver circuit which controls the current flowing through the LEDs to control its brightness. When an LED luminaire is used for communication, the driver circuit is modified (further details in Section V) in order to modulate the data through the use of emitted light. For example, in a simple On-Off Keying modulation, the data bit "0" and "1" can be transmitted by choosing two separate levels of light intensity.

A crucial design requirement for VLC system is that illumination, which is the primary purpose of the LED luminaries, should not be affected because of the communication use. Hence, performance of the VLC system is also affected depending on how the LED luminaires are designed. White light is by far the most commonly used form of illumination in both indoor as well as outdoor applications. This is because colors of objects (also known as color rendering) as seen under the white light closely resemble the colors of the same objects under the natural light. In solid-state lighting, the white light is produced in following two ways -

1) **Blue LED with Phosphor:** In this method, the white light is generated by using a blue LED that has yellow phosphor coating. When the blue light traverses through the yellow coating, the combination produces a white light. Different variations of the white light (color temperatures) are produced by modifying the thickness of the phosphor layer.
2) **RGB Combination:** White light can also produced by proper mixing of red, green and blue light. In this method, three separate LEDs are used which increases the cost of LED luminaire compared to using the Blue LED with Phosphor.

TABLE I
Acronyms and Their Full Names

Acronym	Full form
ACO-OFDM	Asymmetrically-Clipped Orthogonal Frequency Division Multiplexing
ADC	Analog to Digital Converter
AoA	Angle of Arrival
BER	Bit Error Rate
BIBD	Balanced Incomplete Block Designs
CAP	Contention Access Period
CCA	Clear Channel Assessment
CC	Convolutional Coding
CCM	Code Cycle Modulation
CRC	Cyclic Redundancy Check
CSK	Color Shift Keying
CSMA-CA	Carrier Sense Multiple Access - Collision Avoidance
DAC	Digital to Analog Converter
DCO-OFDM	Direct Current biased Optical Orthogonal Frequency Division Multiplexing
DMT	Discrete MultiTone
DOPPM	Differential Overlapping Pulse Position Modulation
DPPM	Differential Pulse Position Modulation
DSRC	Dedicated Short-Range Communication
EPPM	Expurgated Pulse Position Modulation
FEC	Forward Error Correction
FET	Field Effect Transistor
FOV	Field Of View
FPS	frames per second
Gbps	Gigabits per second
GPS	Global Positioning System
GTS	Guaranteed Time Slot
HCI	Human Computer Interaction
HetNets	Heterogeneous Networks
IM/DD	Intensity Modulation/Direct Detection
JT	Joint Transmission
Kbps	Kilobits per second
LCD	Liquid-crystal-display
LED	Light Emitting Diode
LOS	Line Of Sight
LTE	Long Term Evolution
MAC	Medium Access Control
Mbps	Megabits per second
MCS	Modulation and Coding Scheme
MEPPM	Multi-level Expurgated Pulse Position Modulation
MIMO	Multiple Input Multiple Output
MISO	Multiple Input Single Output
MPPM	Multipulse Pulse Position Modulation
MU-MIMO	Multiple User - Multiple Input Multiple Output
NFC	Near Field Communication
NRZ	Non Return to Zero
OCDMA	Optical Code Division Multiple Access
OFDMA	Orthogonal Frequency Division Multiple Access
OFDM	Orthogonal Frequency Division Multiplexing
OMPPM	Overlapping Multipulse Pulse Position Modulation
OOC	Optical Orthogonal Codes
OOK	On Off Keying
OPPM	Overlapping Pulse Position Modulation
PAPR	Peak to Average Power Ratio
PDP	Power Delay Profile
PPM	Pulse Position Modulation
PWM	Pulse Width Modulation
QAM	Quadrature Amplitude Modulation
RC	Repetition Coding
RF	Radio Frequency
RGB	Red Green Blue
RLL	Run Length Limited
RS	Reed-Solomon coding
RSS	Received Signal Strength
RTS/CTS	Request To Send/Clear To Send
SFO	Sampling Frequency Offset
SISO	Single Input Single Output
SLM	Spatial Light Modulator
SMP	Spatial Multiplexing
SM	Spatial Modulation
SNR	Signal to Noise Ratio
VLC	Visible Light Communication
VPPM	Variable Pulse Position Modulation
WDM	Wavelength Division Multiplexing

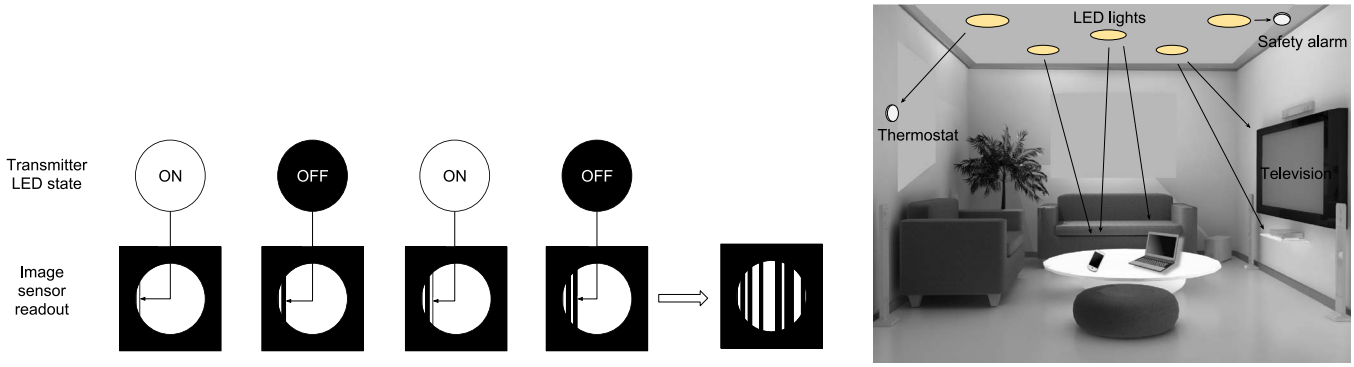

Fig. 2. The rolling shutter effect and typical usage scenario of an indoor VLC network. (a) The rolling shutter effect observed when receiving data using an image sensor. (b) An example scenario showing that LEDs can communicate to various devices including user's mobile devices and other smart devices; reproduced using [15].

Due to ease of implementation and lower cost, the first method with blue LED and phosphor is more commonly used for designing white LED. However, in terms of communication, the phosphor coating limits the speed at which LED can switched to a few MHz. As we will discuss in Section III-B, various solutions have been proposed to alleviate this limitation. On the other hand, RGB combination is preferable for communication as it also creates an opportunity of using Color Shift Keying to modulate the data using three different color wavelength LEDs.

B. VLC Receiver

Two types of VLC receivers can be used to receive the signal transmitted by an LED luminaire

1) **photodetector**—also referred as photodiode or non-imaging receiver,
2) **imaging sensor**—also called a camera sensor.

The photodetector is a semiconductor device that converts the received light into current. The current commercial photodetectors can easily sample the received visible light at rates of tens of MHz.

An imaging sensor or a camera sensor can also be used to receive the transmitted visible light signals. Because such camera sensors are available on most of today's mobile devices like smartphones to capture videos and images, it has the potential to convert the mobile devices in readily available VLC receivers. An imaging sensor consists of many photodetectors arranged in a matrix on an integrated circuit. However, the limitation of an imaging sensor is that in order to enable high-resolution photography, the number of photodetectors can be very high. This significantly reduces the number of frames per second (fps) that can be captured by the camera sensor. For example, the fps of commonly used camera sensors in smartphones is no more than 40. This means that direct use of camera sensor to receive visible light communication can provide very low data rate.

The "rolling shutter" property of camera sensor can be used to receive the data at a faster rate. Due to a large number of available photodetectors in a camera sensor, it is not possible to read the output of each pixel in parallel. Instead modern camera sensors employ row scanning where photodetectors of one row of the matrix is read at a time. This procedure of reading photodetector output row by row (or column-by-column) is referred as rolling shutter. Fig. 2(a) shows how the rolling shutter process can be leveraged to increase the data rate. For illustration purposes, we assume that the transmitter uses ON-OFF modulation. The transmitter can change its state (transmit the next symbol) in a time shorter than the time required to scan a row of pixels. As shown in Fig. 2(a), the transmitter is in ON state first which results in higher intensity output for pixels of the first column. At the next time instance, it changes its state by switching to OFF state. This can be recorded as low intensity output for pixels of the second column. Once all the columns are scanned, all the columns of the resultant image can be converted to binary data. It was shown in [16] that multi-kbps of throughput can be achieved using the rolling shutter process of camera sensor.

Note that image sensor can allow any mobile device with camera to receive visible light communication. However, in its current form, it can only provide very limited throughput (few kbps) due to its low sampling rate. On the other hand, stand-alone photodetectors have shown to achieve significantly higher throughput (hundreds of mbps). In this survey, we assume the receiver to be the photodetector unless otherwise mentioned specifically.

C. VLC Modes of Communication

Visible light communication can be classified into two modes: 1) Infrastructure-to-device communication and 2) Device-to-device communication. An indoor scenario where LED luminaires are used to illuminate the room is shown in Fig. 2(b). In this case, the luminaires can transmit data to various devices inside the room. The LEDs can also coordinate between themselves to reduce the interference and even enable coordinated multi-point transmission to receiving devices. The uplink transmission from the devices are difficult to achieve because using LEDs on end-user devices can cause noticeable disturbance to users. In such case, RF or infrared communication can be used for the uplink transmissions. Similar to the indoor case, the

LEDs used in street lamps as well as traffic lights can be used to provide Internet access to users in cars and pedestrians. We will discuss such vehicular application in Section VI-C.

Due to omni-present camera sensor for mobile devices, the visible light communication can also be used for near-field device-to-device communication. Here, the LED pixels on the display of one smartphone can be used to transmit data to the camera sensor of another smartphone. With recent advances in design of efficient codes, such screen-to-camera streaming has been shown to achieve very high throughput. We discuss these techniques in Section IV-B. In another form of device-to-device communication, cars and other vehicles on the road can communicate with each other to form an ad-hoc network using VLC.

Although we discussed the vehicular networking and screen-camera communication, our primary focus in this survey is towards design and analysis of indoor infrastructure-to-device networking using visible light.

III. Physical Layer

We start with a comprehensive overview of VLC physical layer by discussing 1) channel model and characteristics, 2) modulation methods, and 3) MIMO techniques for VLC.

A. Channel Model and Propagation Characteristics

In this section, we describe the channel model for propagation of visible light. Based on the channel model, it is possible to choose an LED with appropriate specifications and estimate its communication link performance. Note that the notations symbols used throughout this section are listed in Table II with their meaning.

1) Transmitted Power of an LED—Luminous Flux: An LED transmitter serves dual purpose of illumination and communication. Therefore, it is necessary to first establish an understanding of relevant photometric and radiometric parameters. Using these parameters, we will be able to calculate the *Luminous Flux* which is the transmitted power of an LED transmitter. First, we will calculate the transmitted power, path loss and received power of a Line-Of-Sight (LOS) link and then analyze the multipath impact of reflected paths.

Photometric parameters quantify the characteristics of light (such as brightness, color etc.) as perceived by the human eye. They are useful in understanding the illumination aspects of LEDs. *Radiometric parameters* measure the characteristics of radiant electromagnetic energy of light. They are useful in determining communication related properties of LEDs. There are two ways of calculating the Luminous Flux—using spectral integral or using spatial integral. Depending on which parameters are available for a given LED transmitter, one of the two methods can be chosen for calculation of luminous flux.

Spectral Integral: The spectral integral method uses luminosity function of human eye and spectral power distribution of an LED to derive the luminous flux.

Luminosity Function $V(\lambda)$: The *photopic vision* of human eye allows humans to distinguish different colors, making it a crucial factor in designing lighting technology [17]. It was shown in [18] that human's photopic vision exhibits different levels of sensitivity to different wavelengths of visible light spectrum. This aspect is shown in Fig. 3 using the *luminosity function $V(\lambda)$*. The function shows that human eye can see the colors within the range of 380 nm to 750 nm with the maximum sensitivity at wavelength of 555 nm (the yellow-green region).

Spectral Power Distribution $S_T(\lambda)$: The $S_T(\lambda)$ of an LED is the function representing the power of the LED at all wavelengths in the visible light spectrum. The LED vendors typically publish the distribution to explain how different colors will be rendered in the presence of the LED. It is a radiometric parameter measured in Watts/nm. The spectral power distribution of three different colored LEDs are shown in Fig. 4. It can be observed that all three LEDs have high radiant power at two wavelengths—blue and yellow. As described in Section II-A, most current LEDs produce white light by combining blue light emitted by a blue LED with yellow phosphor coating. Depending on the desired type of white color (warm, natural or cool), blue and yellow light emissions are controlled using the

TABLE II
Symbols and Their Meaning

Symbol	Meaning
λ	Wavelength
$V(\lambda)$	Luminosity functiuon
$S_T(\lambda)$	Transmitter spectral power distribution function
F_T	Transmitter luminous flux
F_R	Receiver luminous flux
$g_t(\theta)$	Luminous intensity distribution
I_0	Axial intensity
θ_{max}	Half beam angle
Ω_{max}	Full beam angle
L_L	Luminous path loss
L_P	Optical power path loss
D	Distance between transmitter and receiver
r	Radius of the receiver aperture
α	Incident angle
β	Irradiation angle
A_r	Receiver aperture area
Ω_r	Receiver solid angle from transmitter
m	Order of Lambertial emission
$\phi_{1/2}$	Semi-angle at half illuminance
$R_f(\lambda)$	Spectral responsivity function
P_{R_o}	Received optical power
$S_R(\lambda)$	Receiver spectral power distribution function
λ_{rL}	Lower wavelength cut-off for optical filter
λ_{rH}	Higher wavelength cut-off for optical filter
$P_R(i)$	Received optical power from LOS link of i^{th} LED
$P_R(total)$	Total received optical power
$\rho(\lambda)$	Spectral reflectrance
N	Number of LED transmitters
k	Number of bounces of light
$h(t)$	Power delay profile
δ	Dirac delta function
c	Speed of light
FOV	Acceptance angle of receiver
$\Gamma_n^{(k)}$	Power of reflected ray after k^{th} bounce
σ_{shot}	Standard deviation of shot noise
$\sigma_{thermal}$	Standard deviation of thermal noise
x	Number of photons collected in unit time
κ	Boltzmann's constant
I_B	Photocurrent due to background noise
G_{ol}	Open-loop voltage gain
T_k	Absolute temperature
Cpd	Capacitance of the photodetector per unit area
η	FET channel noise factor
g_m	FET transconductance
I_2, I_3	Noise-bandwidth factors

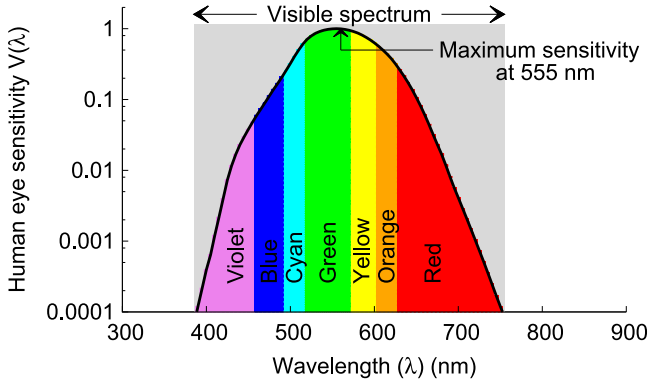

Fig. 3. Luminosity function representing human eye's sensitivity to different wavelengths in the visible spectrum.

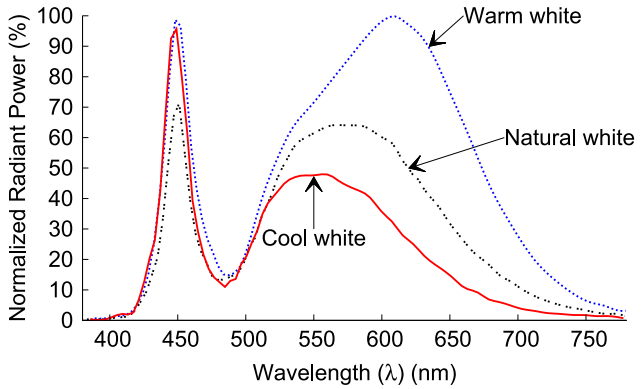

Fig. 4. Power spectral distribution for LED of three color types—warm white, natural white and cool white. Warm white and natural white have more radiated power for green-yellow-orange wavelengths compared to cool white which provides a more bluish illumination; Figure reproduced from [19].

phosphor coating. For example, more yellow light is allowed in warm and natural white compared to the cool white LED.

Luminous Flux: The luminous flux combines luminosity function and spectral power distribution to calculate the "perceived" power emitted by the LED. It weighs the $S_T(\lambda)$ function with $V(\lambda)$ (the sensitivity of human eye to different wavelengths) because we know from Fig. 3 that human eye does not respond to all wavelengths equally. The luminous flux of the transmitter LED (F_T) is measured in lumens and it can be calculated as

$$F_T = 683\ (\text{lumens/watt}) \int_{380\ \text{nm}}^{750\ \text{nm}} S_T(\lambda) V(\lambda) d\lambda. \qquad (1)$$

The constant 683 lumens/watt is the maximum *luminous efficiency*. The luminous efficiency is the ratio of luminous flux to the radiant flux, which measures how well the radiated electromagnetic energy and required electricity of an LED was transformed to provide visible light illumination. We know from Fig. 3 that human eye is most sensitive to detect the wavelength of 555 nm (green). The electrical power necessary to produce one lumen of light at the wavelength of 555 nm is derived to be $1/683^{rd}$ of a watt [20]. This means that for any other color source, the power necessary to produce one lumen of light is always higher than $1/683^{rd}$ of a watt. Hence, the

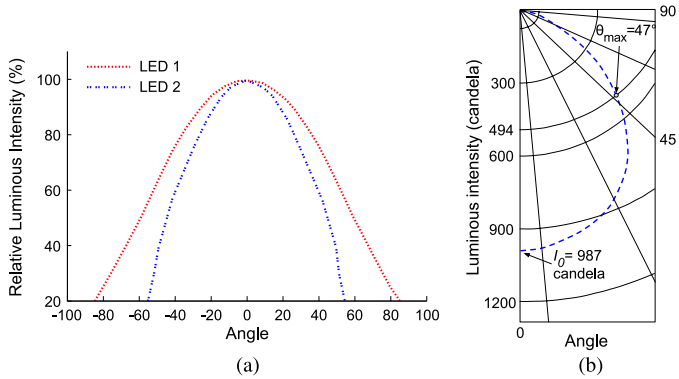

Fig. 5. (a) Luminous intensity distribution for two LED—1) Cree XLamp XP-E High-Efficiency White [19]. 2) Cree XLAMP XR-E [21] (b) Luminous intensity distribution of Cree LMH6 in polar coordinates [22] and its half-beam angle; Figures reproduced from [19]–[22].

maximum luminous efficiency is 683 lumens/watt which occurs at 555 nm wavelength.

Spatial Integral: Another way of calculating the luminous flux is to utilize LED's spatial emission properties. For this, we will use luminous intensity and axial intensity as described next.

Luminous Intensity $g_t(\theta)$: While luminous flux measures the total amount of light emitted by an LED, the luminous intensity measures how bright the LED is in a specific direction. It is measured in Candela which is luminous flux per unit solid angle (1 steradian). This allows us to understand where the LED directs its light. Fig. 5 shows the luminous intensity distribution of three different LEDs. In Fig. 5(a), both the LEDs emit light at wider angles allowing better illumination in many directions, while in Fig. 5(b), it can be observed that LED emits light in a narrower beam (much like spotlighting). Most LED sources have Lambertial beam distribution [23] which means that the intensity drops as the cosine of the incident angle.

There are two important parameters to be derived from the intensity distribution

Axial Intensity (I_0) is defined as the luminous intensity in candelas at 0° solid angle. For LED in Fig. 5(b), the axial intensity is 987 candela. Typically, the luminous intensity distribution provided by the vendors are normalized with the axial intensity as shown in Fig. 5(a).

Half Beam Angle (θ_{max}) is the angle at which the light intensity decreases to half of the axial intensity. For the LED in Fig. 5(b), the half beam angle is 47°. For the Lambertian sources like LEDs, the half beam angle is calculated from the entire beam angle (Ω_{max}) as follows

$$\Omega_{max} = 2\pi(1 - \cos\theta_{max}). \qquad (2)$$

The luminous flux can now be calculated by integrating the luminous intensity function over the entire beam solid angle Ω_{max}. Different from Equ. (1) which was a spectral integral, here the flux is calculated using spatial integral as below

$$F_T = \int_0^{\Omega_{max}} I_0 g_t(\theta) d\Omega \qquad (3)$$

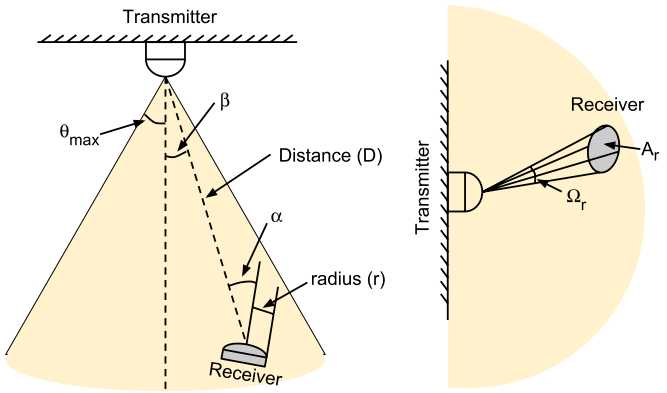

Fig. 6. Relative position of transmitter and receiver in LOS settings; reproduced from [24].

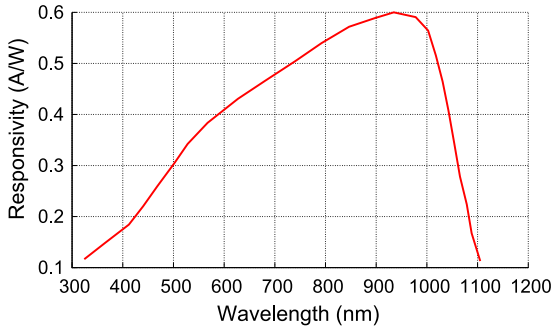

Fig. 7. Spectral response of a typical photodetector receiver; responsivity (measured in A/W) is the ratio of output photocurrent in amperes to incident radiant energy in watts; reproduced from [25].

where $g_t(\theta)$ is the normalized spatial luminous intensity distribution. Combining Equs. (2) and (3), we get

$$F_T = I_0 \int_0^{\theta_{max}} 2\pi g_t(\theta) sin\theta d\theta. \tag{4}$$

2) Path Loss and Received Power: Based on the luminous flux calculated above, we will now derive the value of path loss. It was proven in [24] that the path loss in photometric domain (referred as luminous path loss L_L) is the same the path loss in radiometric domain (referred as optical power path loss L_P). This is due to the fact that in line-of-sight free space propagation, the path loss can be assumed to be independent of the wavelength. Therefore, we can calculate L_L using the luminous flux derived in the previous section. Specifically, L_L is the ratio of luminous flux of the receiver (F_R) and the transmitter (F_T). F_T can be calculated as Equ. (4).

In order to calculate the F_R, it is necessary to specify the relative positions of the transmitter and the receiver. This relative positioning is shown in Fig. 6. Here, the distance between the receiver and the transmitter is D, and radius of the receiver aperture is r. The angle between the receiver normal and transmitter-receiver line is α (also referred as incident angle). The transmitter viewing angle is β (also referred as irradiation angle). Let the receiver solid angle as observed from the transmitter be Ω_r and receiver's area A_r as shown in Fig. 6, then

$$A_r cos(\alpha) = D^2 \Omega_r. \tag{5}$$

From Fig. 6, the receiver flux F_R can be calculated as

$$F_R = I_0 g_t(\beta) \Omega_r. \tag{6}$$

The optical path loss L_L can be calculated using Equations (4), (5), and (6) as

$$L_L = \frac{F_R}{F_T} = \frac{g_t(\beta) A_r cos\alpha}{D^2 \int_0^{\theta_{max}} 2\pi g_t(\theta) sin\theta d\theta}. \tag{7}$$

Most LED sources have Lambertial beam distribution which means that the spatial luminous intensity distribution is a cosine function

$$g_t(\theta) = cos^m(\theta) \tag{8}$$

where m is the order of Lambertial emission. The value of m depends on the semi-angle at half illuminance $\Phi_{1/2}$ of the LED

$$m = \frac{ln(2)}{ln(cos\Phi_{1/2})}. \tag{9}$$

Substituting Equ. (8) and θ_{max} in Equ. (7), we get the path loss value for a Lambertian LED source as follows

$$L_L = \frac{(m+1)A_r}{2\pi D^2} cos\,\alpha\, cos^m(\beta). \tag{10}$$

If the LED emission can not be modeled using the Lambertian cosine function, it is necessary to measure $g_t(\theta)$ for the given LED, and use it to calculate L_L from Equ. (7).

The received optical power can be now calculated using the path loss. It is typical that the receiving photodetector is equipped with an optical filter. Let $R_f(\lambda)$ denote the spectral response of the optical filter. Fig. 7 shows $R_f(\lambda)$ of a typical photodetector. Using $R_f(\lambda)$, the received optical power P_{R_O} for the direct line-of-sight optical link can be calculated as

$$P_{R_O} = \int_{\lambda_{rL}}^{\lambda_{rH}} S_R(\lambda) R_f(\lambda) d\lambda \tag{11}$$

where $S_R(\lambda) = L_P S_T(\lambda) = L_L S_T(\lambda)$ and λ_{rL} and λ_{rH} are lower and upper wavelength cut-off values for the optical filter respectively.

Considering Equations (10) and (11), the received power is dependent on three factors—the transmitter-receiver distance (D), incident angle (α) and irradiation angle (β). These three factors are independent of transmitter and receiver hardware, and depend on receiver's movement and orientation. As an example, if the receiver is a smartphone equipped with a photodiode, the three factors will change based on user's movement and device orientation. It is crucial to understand the impact of these factors on received power in order to evaluate the achievable capacity. Authors in [26] studied the impact using a smartphone

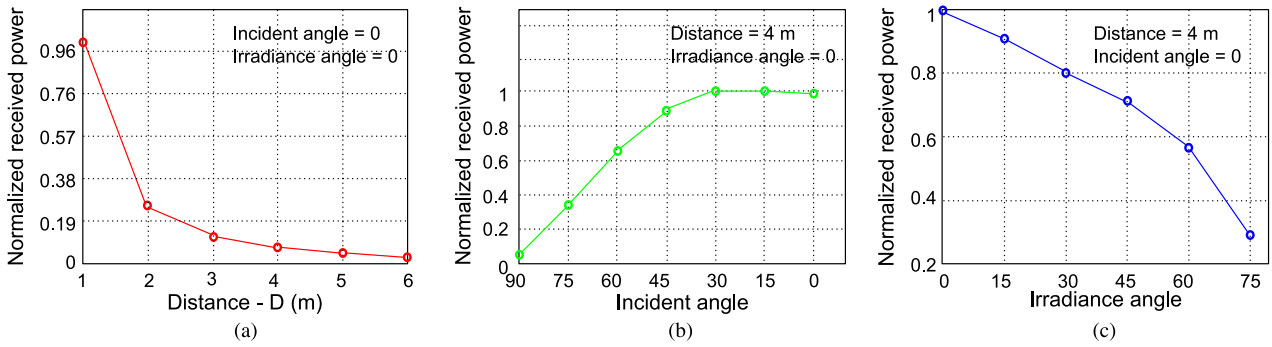

Fig. 8. Impact of (a) transmitter-receiver distance, (b) incident angle (α) and (c) irradiation angle (β) on the received power; reproduced from [26].

photodiode as the receiver. Fig. 8 show how the normalized received power (measured as light intensity on smartphone photodiode) varies with changes in D, α and β. Fig. 8(a) shows how the received power attenuates with D as inverse square low (Equ. (10)). The incident angle measures the changes in smartphone's orientation (0° means photodiode is directly facing the LED). As the incident angle (α) increases, the energy at which the photons strike the photodiode decreases, which in turn results in decrease of received power. Similarly, the received power decreases with increase in the irradiation angle (β) confirming the lambertian emission pattern of the LED. The impact of these three factors have important implications on guaranteeing high SNR in VLC access networks and managing inter-cell interference as we will discuss in Section IV-B.

3) Multipath Propagation With Reflected Paths: As we saw in Section II, typically there are more than one LED in a luminaire. The receiving photodetector can simultaneously receive (intensity modulated) signals from multiple LEDs as shown in Fig. 2(b). The received optical power of the receiver can be calculated by summing the received power of each LOS link within receiver's field-of-view (FOV) can be expressed as

$$P_R(total) = \sum_{i=0}^{N} P_R(i) \tag{12}$$

where N is the total number of LEDs and $P_R(i)$ is the received optical power from LOS link of i^{th} LED calculated from Equ. (11).

Since the majority of the indoor surfaces are more or less reflective of visible light, it is necessary to understand the impact of reflected paths on the performance of communication. Spectral reflectance ($\rho(\lambda)$) represents reflectivity of a surface (such as wall, ceiling etc.) as a function of wavelength. It was noted in [27] that reflectivity of Infrared signal is higher compared to the visible band. The spectral reflectance of commonly used building materials like plaster wall, ceiling etc. was measured in [27] using a spectrophotometer. Fig. 9 shows the results of measured reflectivity. It can be observed that plastic wall has the least reflectivity while the plaster wall has the highest reflectivity.

Because of the reflections, the receiver receives signal from many different paths. Such multipath propagation can be characterized using Power Delay Profile (PDP). The PDP gives the distribution of received power as a function of propagation delay. A non-LOS signal can be bounced from many surfaces

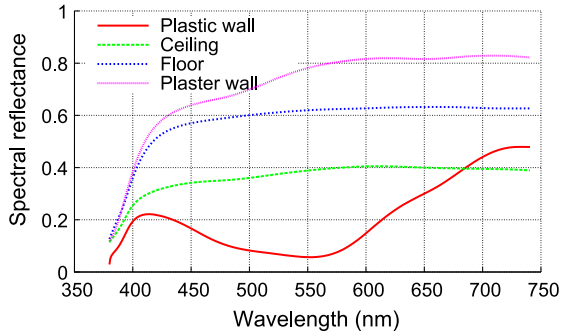

Fig. 9. Different indoor surfaces exhibit different levels of spectral reflectance depending on the wavelength; reproduced from [27].

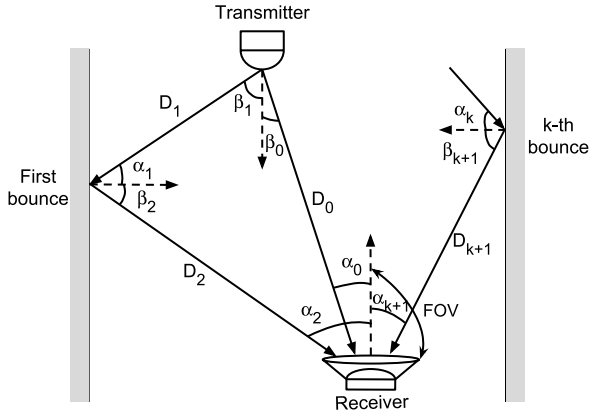

Fig. 10. A non-LOS signal can bounce off the surfaces many times before reaching the receiver; β and α denote the angle of irradiation and incident respectively; reproduced from [27].

before it reaches the receiver photodetector as shown in Fig. 10. Authors in [27] modeled the PDP of multiple bounces for a total of N LEDs at time instance t asd

$$h(t) = \sum_{n=1}^{N} \sum_{k=0}^{\infty} h^{(k)}(t; S_n) \tag{13}$$

where S_n is the spectral power distribution of n^{th} LED and k is the number of bounces. When $k = 0$, the resultant PDP [27] is that of an LOS path as

$$h^{(0)}(t; S_n) = L_0 P_n rect\left(\frac{\alpha_0}{FOV}\right) \delta\left(t - \frac{D_0}{c}\right) \tag{14}$$

where $L_0 = L_L$ is the path loss for the LOS case (derived in Equ. (10)), δ is a Dirac delta function, D_0 is the distance between the LED and the receiver and c is the speed of light. Because the photodiode can only detect the light whose angle of incidence is smaller than its FOV, a rectangular function [27] is used where

$$rect(x) = \begin{cases} 1 & \text{for } |x| \leq 1 \\ 0 & \text{for } |x| > 1 \end{cases}$$

This means that when if a ray does not reach within the FOV of the receiver after k bounces, its effect on the total received power is considered 0.

When $k \geq 1$, the PDP after k bounces (refer Fig. 10) for the n^{th} LED can be calculated [27] as

$$h^{(k)}(t; S_n) = \int_{s \in \mathbb{S}} \left[L_1 L_2 \cdots L_{k+1} \Gamma_n^{(k)} rect\left(\frac{\alpha_0}{FOV}\right) \right. \quad (15)$$

$$\left. \times \delta\left(t - \frac{D_1 + D_2 + \cdots + D_{k+1}}{c}\right) \right] dA_s \quad (16)$$

where

$$L_1 = \frac{A_s(m+1)\, cos\, \alpha_1\, cos^m \beta_1}{2\pi {D_1}^2}. \quad (17)$$

For the path loss of the first bounce L_1, the ray originated from the LED which we have previously modeled as a Lambertian emitter (Equ. (8)). For the remaining bounces, we can calculate the path loss of each path as

$$L_2 = \frac{A_s\, cos\, \beta_2\, cos\, \alpha_2}{\pi {D_2}^2} \quad (18)$$

$$L_{k+1} = \frac{A_R\, cos\, \beta_{k+1}\, cos\, \alpha_{k+1}}{\pi {D_{k+1}}^2}. \quad (19)$$

The integration in Equ. (16) for each surface s of all reflectors $\mathbb{S}$ where A_s is the area of the surface. For L_{k+1}, A_R is the area of the photodiode receiver. $\Gamma_n^{(k)}$ is power of the reflected ray after k^{th} bounce. It is calculated [27] as

$$\Gamma_n^{(k)} = \int_{\lambda} S_n(\lambda) \rho_1(\lambda) \rho_2(\lambda) \ldots \rho_k(\lambda) d\lambda \quad (20)$$

where $\rho_k(\lambda)$ is the spectral reflectance of the surface of k^{th} bounce.

Fig. 11 shows the power delay profile in a realistic scenario where four LED luminaires are deployed in a square topology on a ceiling of a cubic room with either plaster or plastic walls [27]. It can be observed that the first peak is due to the direct received signal (LOS) from the LED. The other peaks are due to multiple reflections from the wall as calculated using Equ. (16). As expected, the received power due to reflection multi-path is relatively lesser compared to the LOS power.

Most of the power delay profiling [27]–[30] of visible light communication rely on simulations. However, detailed measurement-based studies in realistic scenarios (such as indoor places with many different reflecting objects, different LED arrangements etc.) are necessary for improved understanding of multi-path in VLC and developing the techniques to combat it.

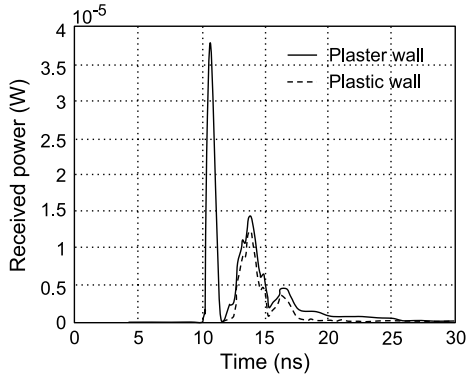

Fig. 11. Power delay profile for 4 LED transmitters in a cubic room with plaster or plastic walls; reproduced from [27].

4) Receiver Noise and SNR: There are three major sources of noise in indoor visible light optical link (1) ambient light noise due to solar radiation from windows, doors etc. and noise due to other illumination sources such as incandescent and fluorescent lamps, (2) shot noise induced in the photodetector by the signal and the ambient light and (3) electrical pre-amplifier noise (also known as thermal noise) of the photodetector.

The ambient noise of solar radiation and artificial illumination sources such as lamps results in ambient noise floor which is a DC interference. The effect of such noise can be mitigated by using a electrical high pass filter at the receiver. Most of the previous studies assume that this ambient noise floor remains stationary over space and time, however, no systematic evaluation is present in the literature. For example, the indoor solar radiation changes at different places depending on windows and doors. The radiation also changes depending on the time of the day (and year) and orientation of the windows/doors. Radiation from other illumination sources will also remain an unavoidable source of noise until we completely transition to LED technology. It is required that exhaustive indoor measurements are carried out to accurately account for such noise.

Once the noise due to solar radiation and artificial illumination sources is filtered, the SNR at the receiver can be calculated based on the shot noise and the thermal noise of the photodetector circuitry as

$$SNR = \frac{{P_{R_E}}^2}{(\sigma_{shot})^2 + (\sigma_{thermal})^2} \quad (21)$$

where σ_{shot} and $\sigma_{thermal}$ are the standard deviation of shot noise and thermal noise respectively. The shot noise is due to inherent statistical fluctuation in the amount of photons collected by the photodetector. It is known that the photon counting follows a poisson distribution which means that if the mean of number of photons collected by the photodetector in a unit time is x, then the standard deviation of number of photons collected is $\sqrt{x}$. This also results in poisson distributed variation in

photoelectrons generated by the photodetector. Based on this, the variance of shot noise can be calculated [23], [31] as below

$$(\sigma_{shot})^2 = 2qP_{R_E}B + 2qI_BI_2B \quad (22)$$

The variance of thermal noise [23], [31] is

$$(\sigma_{thermal})^2 = \frac{8\pi\kappa T_k}{G_{ol}}C_{pd}AI_2B^2 + \frac{16\pi^2\kappa T_k\eta}{g_m}C_{pd}^2A^2I_3B^3 \quad (23)$$

where B Hz is the bandwidth of the photodetector, κ is the Boltzmann's constant, I_B is the photocurrent due to background radiation, G_{ol} is the open-loop voltage gain, T_k is the absolute temperature, C_{pd} is capacitance of the photodetector per unit area, η is the FET channel noise factor, g_m is the FET transconductance, and I_2 and I_3 are the noise-bandwidth factors with values 0.562 and 0.0868 respectively. Shot noise and thermal noise are dependent on the area of the photodetector, and depending on factors such as room temperature, ambient light etc. either of them can dominate the overall noise [23] observed by the VLC receiver.

5) Shadowing: The receiver of a visible light communication link can be shadowed by different objects or humans in the indoor environment. For example, if a receiver photodiode is positioned on a desk, it is possible that movement of the nearby chair can result in shadowing of the receiver. Similarly, if a human passes by frequently between the transmitter and the receiver, the link performance is affected by the frequent shadowing. Authors in [32] studied such case of human mobility using simulations and suggested that in multiple spatially separated LED sources should be used in order to mitigate the frequent disconnections due to human shadowing. Apart from this preliminary work, shadowing in indoor VLC networks is not studied in literature. Given that visible light exhibits significantly different propagation characteristics compared to RF (such as no penetration through walls etc.), it is crucial to characterize and model visible light shadowing in indoor environment. This understanding can also provide insights on deployment aspects of indoor VLC networks and how they should be different than current deployment of LEDs which are primarily used for illumination purposes.

B. Modulation Methods

With the understanding of path-loss, noise and SNR, we now discuss various modulation methods used in VLC. The most striking difference between VLC and RF is that in VLC, the data can not be encoded in phase or amplitude of the light signal [10]. This means that phase and amplitude modulation techniques can not be applied in VLC and the information has to be encoded in the varying intensity of the emitting light wave. The demodulation depends on direct detection at the receiver. These set of modulation techniques are referred as IM/DD (Intensity Modulated/Direct Detection) modulations. In this section, we will discuss the IM/DD modulation techniques used for visible light communication.

Different from other types of communications, any modulation scheme for VLC should not only achieve higher data rate but should also meet the requirements of perceived light to humans. These requirements about perceived light can be characterized by following two properties -

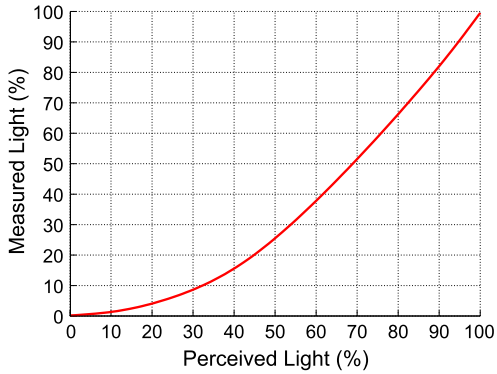

Fig. 12. Human eye perceives the actual measured light differently due to enlargement/contraction of pupil.

(1) Dimming: It was suggested in [17] that different levels of illuminance is required when performing different types of activities. As an example, an illuminance in the range of 30–100 lux is often enough for simple visual tasks performed in most public places. On the other hand, office or residential applications require higher level of illuminance in the range of 300–1000 lux. With the advancements in LED driver circuits, it has become possible to dim an LED to an arbitrary level depending on the application requirement to save energy.

If an LED can be dimmed to an arbitrary level, it is also necessary to understand its impact on the human perceived light. It was first shown in [33] that the relation between the measured light and the perceived light is non-linear. This property is shown in Fig. 12. In other words, a human eye adapts to lower illumination by enlarging the pupil to allow more light to enter the eye. The perceived light can be calculated [33] from the measured light as

$$\text{Perceived light}(\%) = 100 \times \sqrt{\frac{\text{Measured light}(\%)}{100}}. \quad (24)$$

This means that a lamp that is dimmed 1% of its measured light is perceived to be 10% dimmed by the human eye. This is important in terms of VLC because a user may choose an arbitrary level of dimming depending on the application or desired energy savings, but the communication should not be affected by the dimming. In other words, the data should be modulated in such a way that any desired level of dimming is supported.

(2) Flicker mitigation: An additional requirement for any VLC modulation scheme is that it should not result in human-perceivable fluctuations in the brightness of the light. It was shown in [34] that flickering can cause serious detrimental physiological changes in humans. For this reason, it is necessary that changes in the light intensity should happen at a rate faster than human eye can perceive. IEEE 802.15.7 standard [8] suggests that flickering (or change in light intensity) should be

faster than 200 Hz to avoid any harmful effects. This means that any modulation scheme for VLC should mitigate flickering while providing higher data rate.

The most common cause of flickering is long runs of 0s or 1s which can reduce the rate at which light intensity changes and cause the flickering effect. Run Length Limited (RLL) codes are used to mitigate long runs of 0s or 1s. RLL codes ensure that the output symbols have balanced repetition of 0s and 1s. Examples of commonly used RLL codes include Manchester, 4B6B and 8B10B coding. In Manchester coding, a "0" is replaced with a "down" transition ("10") and "1" is replaced with an "up" transition ("01"). 4B6B coding maps a 4 bits symbol to a 6 bits symbol that has balanced repetition. Similarly, 8B10B maps a 8 bits symbol to 10 bits symbol. The number of additional bits added is the highest in the Manchester coding making it a suitable choice for low data rate services that require better balancing. On the other hand, 8B10B reduces the number of additional bits added (high data rate), however, it performs poorly in terms of the DC balancing.

We next discuss four types of modulation schemes used in VLC (1) On-Off Keying, (2) Pulse modulation, (3) Orthogonal Frequency Division Modulation (OFDM) and (4) Color Shift Modulation (CSK). We describe each of them along with a discussion on how they provide the dimming support.

1) On-Off Keying (OOK): In OOK, the data bits 1 and 0 are transmitted by turning the LED on and off respectively. In the OFF state, the LED is not completely turned off but rather the light intensity is reduced. The advantages of OOK include its simplicity and ease of implementation. OOK-like modulation is widely used in wireline communication.

Most of the early work on using OOK modulation for VLC utilize while LED. As we discussed in Section II, such LED produces white light by combining the blue emitter with yellow phosphor. The major limitation of the white LED is its limited bandwidth (few megahertz [35]) due to slow time response of the yellow phosphor. It was first proposed by [36] to use NRZ (Non-Return-to-Zero) OOK with the white LED and a data rate of 10 Mbps was demonstrated over a VLC link. To further improve the performance, [35] used a blue filter to remove the slow-responding yellow component, resulting in a datarate of 40 Mbps. Similarly, [37] and [38] proposed to combine the blue-filtering with analogue equalization at the receiver to achieve data rates of 100 Mbps and 125 Mbps respectively. Authors in [39] showed that the performance can be further improved by using an avalanche photodiode as the receiver instead of the P-I-N photodiode. The achievable data rate with avalanche photodiode and NRZ-OOK was shown to be 230 Mbps. Newly available white LEDs combine the RGB frequencies to produce the white light. The advantage of such LEDs is that they do not have the slow-responding yellow phosphor layer. However, such RGB white LEDs require three separate driver circuits to realize the white light. A different approach was presented in [40] where RGB white LED was used but only the red LED is modulated for data transmission while the other two are provided constant current for illumination. The proposed system can achieve a data rate of 477 Mbps with simple NRZ-OOK modulation and a P-I-N photodiode receiver.

There are two ways proposed in the Standard IEEE 802.15.7 [8] to provide the dimming support when using OOK as the modulation scheme:

1) *Redefine ON and OFF levels:* To achieve the desired level of dimming, the ON and the OFF levels can be assigned different light intensities. The advantage of this scheme is that required level of dimming can be obtained without any additional communication overhead. It can retain the data rate achievable by NRZ-OOK modulation, however, the communication range decreases at lower dimming levels. One major disadvantage is that using lower intensities as ON/OFF levels causes the LEDs to be operated at lower driving currents which in turn has shown to incur changes in color rendering (change in emitted color of LEDs) [41].
2) *Compensation periods:* In this solution, the ON and the OFF levels of the modulation remain the same but additional compensation periods are added when the LED source is fully turned on (called ON periods) or off (OFF periods). The duration of the compensation periods is determined based on the desired level of dimming. Specifically, ON periods are added if the desired level of dimming is more than 50% and OFF periods are added if the desired level of dimming is less than 50%. Authors in [42] proposed a way to calculate the percentage time of active data transmission (γ) within the transmission interval T to obtain a dimming level of D as

$$\gamma = \begin{cases} (2-2D)\times 100 & : D > 0.5 \\ 2D \times 100 & : D \leq 0.5. \end{cases} \tag{25}$$

When the desired dimming level is D with OOK, the maximum communication efficiency E_D can be calculated [42] using information theoretic entropy as

$$E_D = -D\log_2 D - (1-D)\log_2(1-D). \tag{26}$$

This means that communication efficiency is a triangular function of the dimming level with maximum efficiency at dimming level of 50%. The efficiency drops linearly when dimming level decreases to 0% or increases to 100%. The dimming support using compensation periods reduces the data rate, however, since the modulated ON/OFF signals have unchanged intensity, the communication range remains unchanged. To address the problem of lower data rate with compensation periods, [43] proposed to use inverse source coding to maintain the high data rate while achieving the desired level of dimming.

2) Pulse Modulation Methods: Although OOK provides various advantages such as simplicity and ease of implementation, a major limitation is its lower data rates especially when supporting different dimming levels. This has motivated the design of alternative modulation schemes based on pulse width and position which are described next.

Pulse Width Modulation (PWM): An efficient way to achieving modulation and dimming is through the use PWM. In PWM, the widths of the pulses are adjusted based on the

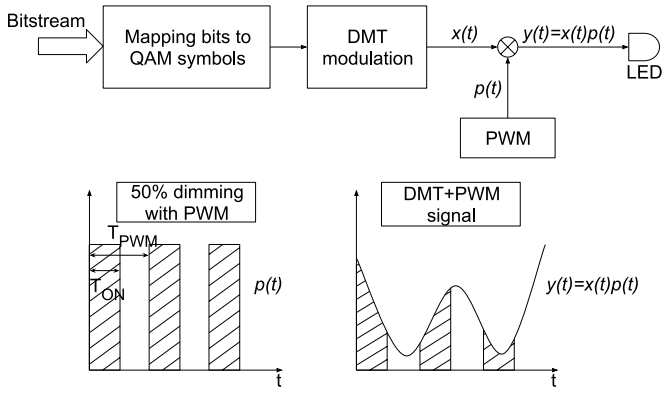

Fig. 13. Transmitter block diagram of DMT transmitter with dimming control (top). An example of how 50% PWM-controlled dimming signal can be combined with a DMT signal as proposed in [44] (bottom); Figures reproduced from [44].

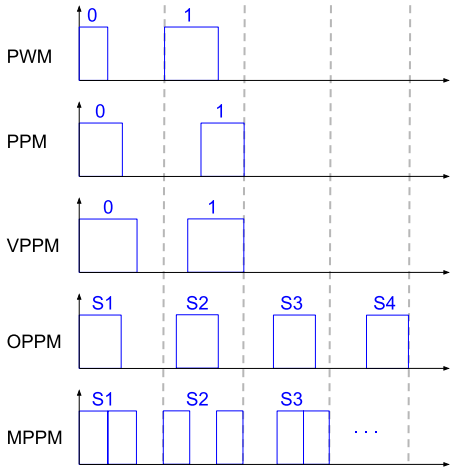

Fig. 14. Schematic diagram showing difference between Pulse Width Modulation (PWM), Pulse Position Modulation (PPM), Variable Pulse Position Modulation (VPPM), Overlapping Pulse Position Modulation (VPPM) and Multipulse Pulse Position Modulation (MPPM); *Sn* refers to nth symbol.

desired level of dimming while the pulses themselves carry the modulated signal in the form of a square wave.

The modulated signal is transmitted during the pulse, and the LED operates at the full brightness during the pulse. The data rate of the modulated signal should be adjusted based on the dimming requirement. Authors in [45] showed that any dimming level from 0% to 100% can be obtained with high PWM frequency. One benefit of PWM is that it achieves the dimming without changing the intensity level of pulses, hence it does not incur the color shift (like OOK with redefined ON/OFF levels) in the LED. The limitation of PWM is its limited data rate (4.8 kbps in [45]). To overcome this limitation, [44] proposed to combine PWM with Discrete Multitone (DMT) for joint dimming control and communication. The approach decouples the dimming based on PWM and communication based on DMT on the transmitter side. As shown in Fig. 13, the bitstream is divided and mapped to symbols using Quadrature Amplitude Modulation (QAM). These QAM symbols are transmitted on different DMT subcarriers that are spaced by $1/T$ in frequency where T is the duration of one symbol. The DMT signal $x(t)$ is combined with PWM square wave signal $p(t)$ where the duty cycle is dependent on desired level of dimming. The resultant signal $y(t) = x(t)p(t)$ is shown in Fig. 13. It was also shown that dimming constraint limits the achievable throughput due to high Bit Error Rate (BER). Authors in [46] also used QAM on DMT subcarriers to achieve a link rate of 513 Mbps, however, it does not address the issue of LED dimming.

Pulse Position Modulation (PPM): Another pulse modulation method in visible light communication is based on the pulse position. In PPM, the symbol duration is divided into t slots of equal duration, and a pulse is transmitted in one of the t slots. The position of the pulse identifies the transmitted symbol. Due to its simplicity, many early designs [47], [48] of optical wireless systems adapted PPM for modulation. In some of the early works of using PPM for infrared communication, authors in [49] proposed the use of rate adaptive transmission scheme where repetition coding is applied to gracefully reduce the throughput in presence of poor channel conditions. Authors in [50] designed a rate-variable punctured convolutional coded PPM for infrared communication. Such a scheme adapts the modulation order of PPM and the code rate of punctured convolutional codes based on the channel conditions. For even worse channel conditions, [51] proposed to use rate adaptive PPM transmission with both repeated and punctured convolutional codes to achieve higher bit rate.

Due to the limitations of lower spectral efficiency and data rate of PPM (only one pulse per symbol duration), other variants of pulse position-based modulation have been proposed over time. A generalization of PPM is referred as Overlapping PPM (OPPM) which allows more than one pulse to be transmitted during the symbol duration [48] and the different pulse symbols can be overlapping (see Fig. 14). [52] showed that OPPM can not only achieve a higher spectral efficiency compared to PPM and OOK but a wide range of dimming levels can be obtained along with the high data rate. Another generalization of PPM was proposed by [53] which is a scheme referred as Multipulse PPM (MPPM). Like OPPM, it allows multiple pulses to be transmitted during the symbol duration, however, the pulses within a symbol duration do not have to be continuous (Fig. 14). It was shown in [48] that MPPM can achieve a higher spectral efficiency compared to OPPM.

Authors in [54] proposed a variation of PPM that combines OPPM and MPPM in a scheme called Overlapping MPPM (OMPPM). In OMPPM, more than one pulse positions are allowed for each optical pulse. It shows that OMPPM can improve the spectral efficiency of MPPM without the expansion of bandwidth in noiseless photon counting channel. Further performance analysis for noisy channels was presented in [55]. It was shown in [56] that OMPPM with fewer pulse slots and more pulses per symbol duration has better cutoff rate performance. Moreover, Trellis-coded OMPPM was studied in [57], [58] to show its effectiveness in direct detection channels with background noise. In another set of modulation scheme, Differential PPM (DPPM) was proposed in [59]. DPPM is similar to PPM except that the OFF symbols after the pulse in a PPM symbol are deleted and the next symbol starts right after the pulse of the previous symbol. It was shown in [48] that DPPM requires significantly less average power than PPM for a given

bandwidth in an optical communication channel. Authors in [60] proposed Differential Overlapping PPM (DOPPM) where differential deletion of OFF symbols is applied to OPPM, and showed that it achieves better spectral efficiency and cutoff performance than PPM, DPPM and OPPM.

Authors in [61] proposed EPPM (Expurgated PPM) where symbols in the MPPM are expurgated to maximize the inter-symbol distance. EPPM achieves the same spectral efficiency as PPM, however, it can be used in VLC to provide dimming support as it can achieve arbitrary level of illumination by changing the number of pulses per symbol (code-weight) and the length of the symbol (code-length) [62]. With many pulses in a symbol, EPPM can also mitigate the flickering as compared to PPM. MEPPM (Multi-level EPPM) [63] extends the EPPM design with support to multiple amplitude levels in order to increase the constellation size and spectral efficiency. MEPPM can also support the dimming and provides flicker-free communication. IEEE 802.15.7 [8] standard proposes a pulse modulation scheme called Variable PPM (VPPM) which is a hybrid of PPM and PWM. In VPPM, the bits are encoded by choosing different position of pulse as in PPM, however, the width of the pulse can also be modified as needed. VPPM retains the simplicity and robustness of PPM while allowing different dimming levels by altering the pulse width.

3) Orthogonal Frequency Division Multiplexing (OFDM): One limitation of previously discussed single-carrier modulation schemes is that they suffer from high inter-symbol interference due to non-linear frequency response of visible light communication channels. OFDM has been widely adopted in the RF communication due to its ability to effectively combat the inter-symbol interference and multipath fading. Authors of [64] first proposed the use of OFDM for visible light communication. In OFDM, the channel is divided into multiple orthogonal subcarriers and the data is sent in parallel sub-streams modulated over the subcarriers. OFDM for VLC can reduce the inter-symbol interference and does not require complex equalizer, however, there are multiple challenges in realizing its implementation. First, the OFDM technique for RF needs to be adapted for application in IM/DD systems such as VLC. This is because OFDM generates complex-valued bipolar signals which need to converted to real-valued signals. This can be achieved by enforcing Hermitian symmetry constraint on the sub-carriers and then converting the time-domain signals to unipolar signals.

Depending on how the bipolar signals are converted to unipolar, there are two types of OFDM techniques: 1) Asymmetrically-Clipped Optical OFDM (ACO-OFDM) and 2) DC-biased Optical OFDM (DCO-OFDM). In ACO-OFDM, only odd subcarriers are modulated [65] which automatically leads to symmetric time domain signal. While in DCO-OFDM [64], [66], [67], all subcarriers are modulated but a positive direct current is added to make the signal unipolar. [68] presented a comparison of both the OFDM schemes and showed that LED clipping distortion is more significant in DCO-OFDM compared to ACO-OFDM. The biggest challenge in OFDM VLC system is the non-linearity of LED [69] which is that the relationship between the current and the emitted light of the LED is non-linear. This especially affects the OFDM-based VLC systems which have higher Peak-to-Average Power Ratio (PAPR). The effect of this non-linearity was studied in [70], [71] and a solution was proposed to combat it by operating the LED in a small range where the driving current and optical power are quasi-linear. Apart from the non-linearity, there is only a limited support for dimming [72] in OFDM-based modulation schemes. Despite these challenges, OFDM for VLC holds great potential with achievable link rates in the scale of multiple gbps [73], [74] using only single LED.

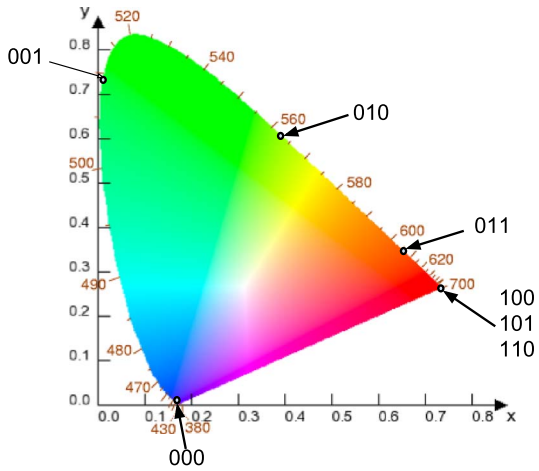

Fig. 15. CIE 1931 chromaticity diagram; The seven color codes correspond to the centers of seven bands dividing the visible spectrum as shown in Table III; reproduced from [81].

TABLE III
THE SEVEN BANDS USED IN CSK AND THEIR CODE, CENTER AND CHROMATICITY COORDINATES

Band (nm)	Code	Center (nm)	(x, y)
380-478	000	429	(0.169, 0.007)
478-540	001	509	(0.011, 0.733)
540-588	010	564	(0.402, 0.597)
588-633	011	611	(0.669, 0.331)
633-679	100	656	(0.729, 0.271)
679-726	101	703	(0.734, 0.265)
726-780	110	753	(0.734, 0.265)

TABLE IV
VALID COLOR BAND COMBINATIONS THAT CAN BE CHOSEN FOR BUILDING THE CONSTELLATION TRIANGLE FOR CSK

	Band i	Band j	Band k
1	110	010	000
2	110	001	000
3	101	010	000
4	101	001	000
5	100	010	000
6	100	001	000
7	011	010	000
8	011	001	000
9	010	001	000

4) Color Shift Keying (CSK): To overcome the lower data rate and limited dimming support issues of other modulation schemes, IEEE 802.15.7 standard [8] proposed CSK modulation which is specifically designed for visible light communication. CSK has attracted increasing amount of attention from research community in last couple of years [75]–[80]. As we

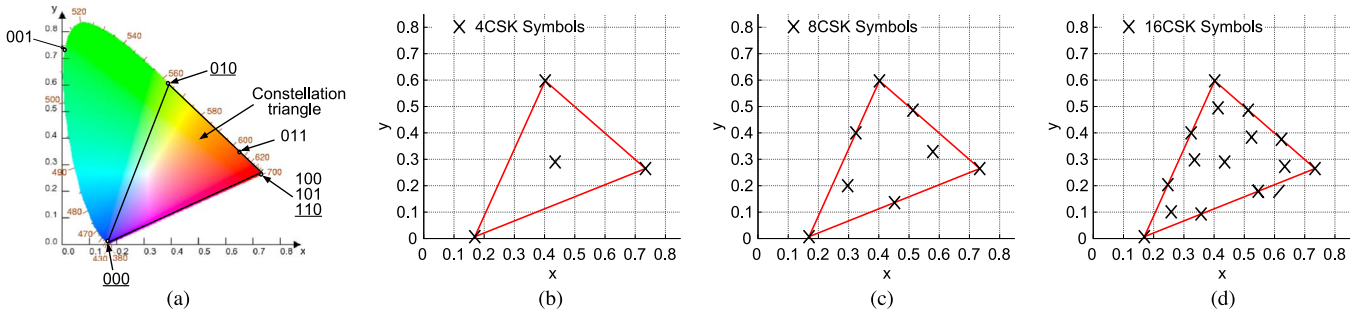

Fig. 16. (a) RGB constellation triangle (110, 010, 000) (b-d) Symbols of 4-CSK, 8-CSK and 16-CSK.

discussed before, generating white light using blue LED and yellow phosphorus slows down the fast switching ability of LED and hinders high data rate communication. An alternative way to generating white light which is recently becoming more and more popular is to utilize three separate LEDs—Red, Green and Blue (RGB). This combined source with RGB LEDs is often referred as TriLED (TLED). CSK modulates the signal using the intensity of the three colors in the TLED source.

CSK modulation relies on the color space chromaticity diagram as defined by CIE 1931 [18] (see Fig. 15). The chromaticity diagram maps all colors perceivable by human eye to two chromaticity parameters—x and y. The entire human visible wavelength is divided into seven bands as shown in Table III and their centers are marked in Fig. 15. Based on the diagram, the CSK modulation [8], [80] is performed as follows

1) **Determine RGB constellation triangle:** The constellation triangle is decided based on the center wavelength of the three RGB LEDs used in the TLED source. Table IV shows the valid color band combinations as proposed by [80] that can be chosen as the constellation triangle depending on the central wavelength of the RGB LEDs. For the purpose of illustration, let us assume that we choose the CSK constellation triangle to be (110, 010, 000) as shown in Fig. 16(a) (example adapted from [80]).
2) **Mapping data bits to chromaticity values:** Depending on 4CSK, 8CSK or 16CSK being used, the chromaticity values of symbols can be derived from the constellation triangle. For our example, Fig. 16(b)–(d) show how data bits can be represented using the symbols for 4CSK, 8CSK and 16CSK. Determining the position of the symbols in the constellation design requires solving an optimization problem where the distance between the symbols should be maximized to minimize the inter-symbol interference. Note that there is an additional constraint in the problem which ensures that the symbols should be equally distributed in the triangle so that the combined light emitted when transmitting different symbols is perceived by the human eye to be white light only. The optimization problem has been studied in [75]–[78] as we discuss next. Once the symbol coordinates are decided, each symbol is assigned a bit sequence (e.g. in 4CSK, the 4 symbols are assigned 00, 01, 10 and 11 respectively), which is then used to map the incoming bits to the symbols.
3) **Determine the intensities of RGB LEDs:** The symbols are transmitted by varying the intensities of the RGB LEDs. The individual intensities of the three LEDs (P_i, P_j and P_k) for each symbol is calculated by solving the following equations:

$$x_s = P_i x_i + P_j x_j + P_k x_k \tag{27}$$
$$y_s = P_i y_i + P_j y_j + P_k y_k \tag{28}$$
$$P_i + P_j + P_K = 1 \tag{29}$$

where x_s and y_s are the chromaticity values of the symbol (Fig. 16), and (x_i, y_i), (x_j, y_j) and (x_k, y_k) are the chromaticity values of the central wavelength of the RGB LEDs being used (three points of the constellation triangle). The receiver uses the R, G and B intensities to decode the transmitted signal.

Dimming support in CSK is simply amplitude dimming where the driving current of the LEDs is varied to change the brightness of resultant white light. Also, different from OOK and pulse modulations, flickering is not a problem with CSK since no amplitude variation is employed. Due to these advantages, researchers have recently attempted to improve the CSK scheme of IEEE 802.15.7 by designing its generalized forms with arbitrary constellation. Authors in [75] presented a CSK constellation design technique based on Billards equivalent disk packing algorithm. Similarly, [76] and [77] developed similar techniques with the use of different optimization algorithms such as interior point methods. All the constellation design techniques are designed to meet the color balance requirement where the TLED source is required to produce any desired color for illumination. The use of four LEDs (blue, cyan, yellow and red) was suggested in [78]. With four LEDs, it is possible to achieve a quadrilateral constellation shape that allows QAM-like constellation design. The presented system is shown to be more energy efficient as well as reliable (less inter-symbol noise) compared to the conventional CSK with 3 LEDs.

The RGB tri-LED can also be used to implement Wavelength Division Multiplexing (WDM)—a multiplexing technique commonly used in fiber optics communication. Authors in [82] proposed modulating separate data streams on three colors which together multiplex to white light. With the use of DMT, an aggregate data rate of 803 Mbps was shown to be achievable using single RGB LED in [82]. Authors in [83] proposed the use of carrier-less amplitude and phase modulation on WDM VLC system with RGB LED to achieve a data rate of 3.22 Gbps.

TABLE V
802.15.7 PHY I OPERATING MODE SPECIFICATIONS AND ACHIEVABLE THROUGHPUT

MCS	Modulation	RLL code	Optical clock rate	FEC		Data rate (kbps)
				Outer code (RS)	Inner code (CC)	
0	OOK	Manchester	200 KHz	(15,7)	1/4	11.67
1				(15,11)	1/3	24.44
2				(15,11)	2/3	48.89
3				(15,11)	none	73.3
4				none	none	100
5	VPPM	4B6B	400 KHz	(15,2)	none	35.56
6				(15,4)	none	71.11
7				(15,7)	none	124.4
8				none	none	266.6

TABLE VI
802.15.7 PHY II OPERATING MODE SPECIFICATIONS AND ACHIEVABLE THROUGHPUT

MCS	Modulation	RLL code	Optical clock rate	FEC	Data rate (Mbps)
16	VPPM	4B6B	3.75 MHz	RS(64,32)	1.25
17				RS(160,128)	2
18			7.5 MHz	RS(64,32)	2.5
19				RS(160,128)	4
20				none	5
21	OOK	8B10B	15 MHz	RS(64,32)	6
22				RS(160,128)	9.6
23			30 MHz	RS(64,32)	12
24				RS(160,128)	19.2
25			60 MHz	RS(64,32)	24
26				RS(160,128)	38.4
27			120 MHz	RS(64,32)	48
28				RS(160,128)	76.8
29				none	96

TABLE VII
802.15.7 PHY III OPERATING MODE SPECIFICATIONS AND ACHIEVABLE THROUGHPUT

MCS	Modulation	Optical clock rate	FEC	Data rate (Mbps)
32	4 CSK	12 MHz	RS(64,32)	12
33	8 CSK		RS(64,32)	18
34	4 CSK	24 MHz	RS(64,32)	24
35	8 CSK		RS(64,32)	36
36	16 CSK		RS(64,32)	48
37	8 CSK		none	72
38	16 CSK		none	96

IEEE 802.15.7 Physical Layer IEEE 802.15.7 [8] standard has specified three PHY layers for VLC with a total of 30 MCS (Modulation and Coding Scheme) indexes. These MCS levels are shown in Tables V–VII. Both PHY I and PHY II utilize OOK and VPPM for modulation. PHY I utilizes Reed Solomon (RS) and Convolutional Codes (CC) for Forward Error Correction (FEC), while PHY II and III mostly reply for RS codes only for FEC.

As described in [79], "optical clock rate" is an important parameter for the performance of the PHY layers. PHY 1 utilizes lower optical rate of $\leq$ 400 KHz. This is because PHY 1 is designed to be usable in outdoor scenarios as well where the LED transmitters are typically high-power and can switch the intensity at a slower rate. PHY II is designed to be used indoors where the optical switching rate can be as high as 120 MHz. The optical rate is 24 MHz for PHY III which is the current feasible switching rate for white TriLED.

Depending on the choice of modulation, RLL code, optical clock rate, FEC code, the three PHY modes can provide different data rates. PHY I can provide data rates from 11.67 Kbps upto 266.6 Kbps. PHY II can achieve data rates from 1.25 Mbps upto 96 Mbps. PHY III can yield data rates starting from 12 Mbps upto 96 Mbps. Further details of physical layer of IEEE 802.15.7 are provided in [79].

Table VIII provides a comparison between four major modulations schemes proposed for VLC. It can be observed that OFDM and CSK are more suitable for high data-rate applications in VLC access networks. As we will discuss next, OFDM is also more suitable for VLC MIMO design, however, more research is necessary to ensure dimming support in OFDM. Another advantage of CSK is that it can provide multi-user access through wavelength multiplexing as we will discuss in Section IV. Increasing demand of higher data-rates is likely to drive further research and development of OFDM and CSK for VLC-based access networks.

C. Multiple Input Multiple Output (MIMO)

In order to provide sufficient illumination, most of the luminaires typically contain multiple LEDs. These multiple LEDs can be treated as multiple transmitters that can enable visible light MIMO communication. In RF communications, MIMO systems are commonly used (in IEEE 802.11n, Long-Term Evolution—LTE) to obtain higher data rates. Similarly, multiple LEDs can be used for higher spectral efficiency in VLC. Note that there are certain similarities between the VLC MIMO systems discussed in this section and screen-camera links (discussed in Section VI-B) as both of them can use an image sensor as a MIMO receiver. The difference is that unlike smartphone screens, the multiple LED transmitters considered here are also used for the illumination. We will provide further details of the screen-camera links in Section VI-B.

MIMO systems in VLC are difficult to realize compared to RF communications. In RF MIMO systems, the throughput gains are largely attributed to spatial diversity (existence of multiple spatial paths that are diverse in nature). However, such diversity gains are limited in VLC MIMO because paths between the transmitter and receiver are very similar (less diverse) especially in indoor scenarios. This limits the available spatial diversity of VLC MIMO systems. The other challenge in VLC MIMO is the design of the receiver as we discuss next.

1) MIMO Receiver: As we discussed in Section II, there can be two types of receivers in VLC MIMO systems—photodiode and image sensor. The performance of the system depends on whether imaging (image sensor) or non-imaging (photodiode) receiver is used [84].

TABLE VIII
MAJOR MODULATION SCHEMES AND THEIR CHARACTERISTICS

Modulation	Data Rate	Dimming Support	Flickering Issue	Comments
OOK	Low to moderate	Yes	High	Low-complexity transceiver design
PPM	Moderate	Yes	Low	Maximum spectral efficiency with MEPPM
OFDM	High	No	Low	Complex design due to LED non-linearity, MIMO support
CSK	High	Yes	Low	Requires RGB tri-LED, improved multi-user access

Non-imaging receiver in a MIMO system is a set of *independent* photodiodes each with its individual concentrator optics. The advantage of such a receiver is that a very high gain can be achieved due to narrow FOV of each photodiode. The disadvantage, however, is that such a receiver requires careful alignment with the transmitters because of the narrow FOV, and the capacity can reduce dramatically even with minor misalignment.

Imaging Receiver: Since an image sensor contains a projection lens and a large matrix of photodiodes, it has the potential to create a high data-rate MIMO link. The projection lens ensures a large FOV which nearly eliminates the alignment requirement. The disadvantage of such as a receiver is that individual photodiodes have limited gain and advance image processing is required to create an efficient MIMO channel. Also, the sampling rate of the image sensor is comparatively lower further reducing the achievable throughput.

The channel models of both imaging and non-imaging receiver MIMO, and their relative benefits and limitations were presented in [84]. It was shown in [85] that an "ideal" MIMO receiver can be a hybrid of imaging and non-imaging sensors which can achieve high gains of LOS paths using narrow FOV like photodiodes and can be robust by leveraging non-LOS paths whenever needed like an image sensor. Authors in [86] proposed the design of a spherically-shaped receiver that is made of a large number of photodiodes. Each of the photodiode has a narrow FOV and points in different direction in the room. The photodiodes pointing to transmitter LED can receive the signal with high gain while other photodiodes pointing to other directions can establish non-LOS channels to increase spatial diversity. However, using such a receiver incurs cost for additional hardware. Instead, authors in [87] proposed a way to improve the lower sampling rate of the image sensor. A token-based pixel selection method was proposed where instead of conventional row-scanning approach, only the pixels of interest are selectively scanned to improve the sampling rate.

2) VLC MIMO Techniques: There are three types of VLC MIMO techniques proposed in literature [88].

Repetition Coding (RC): This is the simplest technique where the same signal is transmitted from all the transmitters. The transmitted signal from all LEDs meet constructively at the receivers increasing the overall gain.

Spatial Multiplexing (SMP): In SMP, different data is transmitted from each transmitter to a receiver photodiode. With multiple transmitters and receivers, this type of MIMO creates multiple parallel SISO streams. The challenge is that receiver photodiodes have to be accurately aligned to the transmitters to avoid any inter-channel interference. SMP MIMO for optical channels has been studied in some of the early works [89]–[91]. In [89], [91], authors proposed optical wireless MIMO communication with subcarrier multiplexing where zero forcing was utilized to cancel the interference from other transmit antennas. It was shown that for the transmitter semi-angle more than 20°, the transmitter-receiver separation should be more than 1.5 meters for lower BER. The impact of optical beat interference on OMIMO scheme of [89] was studied in [90]. Optical beat interference is the signal degradation caused by multiple transmitters transmitting simultaneously on nearby wavelengths.

Spatial Modulation (SM): This MIMO technique was proposed by [92]–[95] where only one transmitter transmits data at any point of time. The constellation diagram is extended to include the spatial dimension. Each transmitter LED is assigned a specific symbol and when data bits to be transmitted matches the symbol, the LED is activated. The receiver estimates which LED was activated based on the received signal, and uses this to decode the transmitted data. Since the data is encoded in both spatial and signal domain, SM achieves much higher spectral efficiency compared to other techniques.

A comparison of all the three MIMO techniques were provided in [88]. It was shown that RC is less restrictive in terms of its requirement for transmitter-receiver alignment but provides only a limited spectral efficiency. SMP, on the other hand, requires more careful alignment of transmitter-receiver but also provides higher data rates compared to RC. SM achieves the best of both worlds by being robust to correlated channels and providing higher spectral efficiency. Also, it was shown in [96] that imaging receivers can obtain much higher SNR when using SM or SMP technique compared to the non-imaging receivers.

Due to its advantages over other MIMO techniques, SM has been studied further in recent years. It was shown in [97], [98] that power imbalance between the transmitter LEDs can improve the performance of spatial modulation especially when optical paths between the transmitter and receiver are highly correlated. Authors in [99] studied the performance of spatial modulation using an implementation of 4×4 MIMO system and showed that the challenge in achieving higher throughput with SM is to maintain symbol separation in the constellation from the receiver's perspective. Researchers investigated the performance of spatial modulation in [100] when only partial channel state information (CSI) is available and concluded that highly accurate CSI estimation is necessary to realize the full potential of SM. The use of generalized spatial modulation was proposed in [97], [101]. Such modulation extends the original scheme by allowing more than one transmitter to be active during the a symbol duration. It was shown that due to additional flexibility of activating multiple LEDs, the generalized scheme can achieve higher spectral efficiency compared to the conventional scheme, however, at the cost of additional complexity in constellation design.

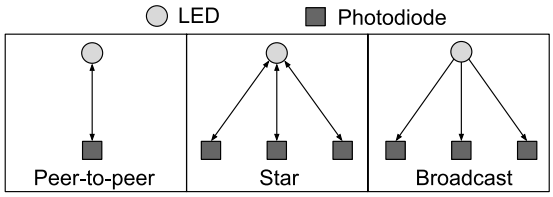

Fig. 17. VLC link layer topologies; reproduced from [8].

Optical MIMO for non-LOS diffuse links has not received much attention. Authors in [102] showed how backward spatial filter can be used for optical wireless MIMO in diffuse channels (no precise alignment of transmitter and receiver). With user movements, such diffuse channel are more likely in practical scenarios and optimizing MIMO performance for such channels should be investigated further.

3) Optical Beamforming: Beamforming allows multiple transmitters to concentrate their signal in a specific direction based on the receiver location. This type of transmit beamforming is well studied in RF communication and also utilized by recent WLAN standards such as IEEE 802.11ac. Similar to RF beamforming, emitting light from multiple LEDs can be focused towards the receiver to create optical beamforming. Recently, it was shown in [103] how light emitted from a single LED can be focused in a specific target direction using Spatial Light Modulator (SLM). SLM is an additional device that is required to modulate the phase or amplitude of the visible light signal. It was shown that significant SNR improvements can be achieved by using the optical beamforming with any modulation technique. Authors in [104] derived the transmit beamforming vectors when multiple LEDs are used to perform the optical beamforming. Optical beamforming can improve the performance of a visible light communication link significantly, however, there is only a limited amount of research done towards this. Performing optical beamforming while meeting the illumination constraints is an important direction for research in VLC MIMO systems.

IV. Link Layer

When there exists multiple transmitter LEDs and receiver devices connected to them, it is essential to control the medium access, device association and device mobility. In this section, we provide an overview of different techniques proposed in literature to manage link layer services.

A. Medium Access Control (MAC)

The application scenarios of VLC can be used to identify the link layer topologies that need to be supported by the MAC protocols. IEEE 802.15.8 [8] proposes three types of link layer topologies for VLC as shown in Fig. 17.

1) **Peer-to-peer:** The peer-to-peer topology involves one device acting as a coordinator (or master) for the link between two devices. Both devices can communicate with each other since the client has an uplink to the master. This topology is typically more suitable for high-speed Near-Field Communication (NFC).
2) **Star:** In a start topology, there can be many client devices connected to a master device which acts as the coordinator. A typical use case of this topology is VLC wireless access networks. The MAC design is especially challenging in the star topology due to many bi-directional links in the same collision domain.
3) **Broadcast:** Different from the star topology, the client devices in a broadcast topology can only receive data from the master LED transmitter without forming any uplink. Such topology can be used for broadcasting information via LEDs throughout the network. Since there is no explicit association needed, the broadcast topology simplifies the MAC design.

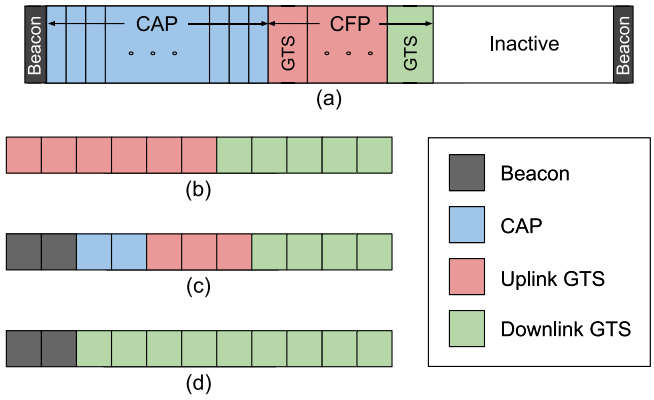

Fig. 18. (a) IEEE 802.15.7 frame structure includes beacon, Contention-based Access Periods (CAP) and Contention Free Periods (CFP). (b)–(d) Example usage of frame structure in different topologies; reproduced from [8].

Three types of multiple access control (MAC) schemes are proposed for VLC—Carrier Sense Multiple Access (CSMA), Orthogonal Frequency Division Multiple Access (OFDMA) and Code Division Multiple Access (CDMA).

CSMA: There are two types of random channel access mechanisms proposed by IEEE 802.15.7 standard. In the first type, the beacons from the coordinator are disabled. Such beacon-disabled random access uses an unslotted random channel access with CSMA. Here, if a device wishes to transmit, it first waits for a random back-off period and then senses the channel to be busy or not, before transmitting. If the channel is found to be busy, the device waits for another random period before trying to access the channel again. In the second type where the beacons are enabled, the time is divided into beacon intervals. A superframe within the beacon interval contains Contention Access Periods (CAP) and Contention Free Periods (CFP) as shown in Fig. 18(a). If a device wishes to transmit, it first locates the start of a next back-off slot and then waits for a random number of back-off slots before performing Clear Channel Assessment (CCA). If the channel is found to be idle, the device starts to transmit. If the medium is found to be busy, the device waits for additional random number of back-off slots before performing the CCA again.

The beacon-enabled random access also contains contention free period which consists of multiple Guaranteed Time Slots

(GTS). This period is used by the coordinator to ensure medium access to devices with delay or bandwidth constrained applications. Depending on the requirement, a coordinator can also assign multiple time slots to one GTS. Fig. 18(b)–(d) show how different types of slots are used for beacon-disabled access in peer-to-peer topology, beacon-enabled access in star and broadcast topologies respectively.

A preliminary version of CSMA/CA-based MAC was implemented on a testbed by [105] with OOK modulation. The CSMA/CA implementation was extended in [106] for cases where different LED transmitters have different FOV. It shows that when transmitters are heterogeneous, avoiding collisions especially due to hidden terminals is a challenging problem. It provides design and implementation of Request-To-Send/ Clear-To-Send (RTS/CTS) on OpenVLC platform (discussed in Section V). Authors observe that when an LED OFF symbol (logic "0") is being transmitted by an LED transceiver A, the receiver node B can use the same optical channel to transmit information to the LED A at the same time, enabling a bidirectional communication.

OFDMA: OFDMA is a multi-carrier multiple access scheme where different users are assigned separate resource blocks (set of subcarriers in time) for communication. Application of OFDMA for multiple access in VLC is a natural extension to utilizing OFDM for modulation in physical layer. Two variations of OFDMA were compared in [107] and it was shown that power efficiency and decoding complexity are two main challenges while applying OFDMA to VLC. Authors in [108] proposed a heuristic solution to subcarrier allocation problem in the case of interfering transmitters. Considering the spectral efficiency of OFMA, further research is necessary to design power-efficient and interference-aware resource allocation schemes for OFDMA. Authors in [109] proposed to use joint transmission from multiple LEDs using OFDMA to improve the SINR of the edge users in a room. It was shown that due to intensity modulation of VLC systems, it is possible to achieve much better coordinated multi-point transmission compared to RF systems.

CDMA: Optical CDMA (OCDMA) relies on optically orthogonal codes to provide access to the same channel by multiple users. The principle of optically orthogonal codes is well-studied for the optical fiber networks [110], [111]. In the OCDMA for VLC, each device is assigned a code (binary sequence) such that the data can be encoded in time domain by turning the LED ON and OFF [112]. These codes are referred as Optical Orthogonal Codes (OOC) [110]. It was shown in [112] synchronous OCDMA can be implemented using the OOC codes and OOK modulation with LED transmitters. A limitation of this technique is that long OOC codes are needed to ensure optimality, which in turn reduces the achievable data rate of devices. Authors in [113] proposed to address this issue using Code Cycle Modulation (CCM) where different cyclic shifts of the sequence assigned to devices are used to transmit an M-ary information. Since any cyclic shift of an OOC code (with length L) is considered a symbol, the spectral efficiency increases by a factor of $\log_2 L$.

Authors in [114], [115] showed that the CCM OOC codes can provide higher spectral efficiency, however, they are not suitable for providing dimming support. This is because to achieve a different dimming level (different Peak-to-Average-Power-Ratio (PAPR)), a new set of OOC codes are required to be calculated. Two techniques have been proposed to address this issue in [114] and [115]. In the first method, user's encoded binary sequence is multiplied by BIBD (Balanced Incomplete Block Designs) codewords, and the results are added to generate a Multi-level MEPPM signal. This way, the dimming level can be changed by changing the ratio of code-length to code-weight of the BIBD code, without changing the OOC codes. In the second technique, the BIBD codes are partitioned in different subsets for different devices. The MEPPM scheme is used to generate multi-level signals based on the assigned subsets. Since this technique provides larger constellation size, it can ensure higher data rate for each user.

It was also identified in [116] that when there are a large number of devices sharing the channel access, the OOC codes are difficult to generate. This has led to design of random optical codes [116]. It was shown that the random codes are not optimal, however, their ease of generation and ability to support a large number of users in multiple access make them a valid alternative. The performance of the random codes was studied in [117] where the limits of their spectral efficiency was also demonstrated. It was shown in [118] that the reflected light inside a room can increase the inter-symbol interference of the OCDMA system, and the performance degrades furthermore as the number of users increase in the system. When utilizing optical CDMA for multi-user access, authors in [119] proposed a centralized power allocation algorithm that maximizes the minimum SINR (Signal to Noise and Interference Ratio) of all devices. This centralized algorithm achieves improved BER performance, however, it requires all the LED transmitters to communicate with each other, which might not be scalable due to its computational complexity in a large indoor environment with many LEDs and receivers.

Recently, CSK modulation with RGB tri-LED transmitter has been combined with OCDMA to achieve multi-user VLC. [120] and [121] showed how different CSK symbols can be combined with the CDMA codes of users to simultaneously transmit data to multiple devices. Lastly, authors in [122] proposed a hybrid CDMA and OFDM scheme that can achieve the advantages of both as previously suggested for RF communication in [123].

Multi-User MIMO (MU-MIMO): Advanced MIMO techniques such as Multi-user MIMO (MU-MIMO) are still to be designed and developed for VLC. Some early work such as [124] studied the multi-user MISO (Multiple Input Single Output) problem where multiple transmitter LEDs (connected via power-line network in indoor environment) can coordinate to transmit the data to different users while canceling the inter-user interference using zero-forcing pre-coding. Authors in [125] designed a precoding MU-MIMO VLC system where block diagonalization algorithm was adopted to eliminate multi-user interference. It showed that such precoding reduces the receiver-side computational complexity and power consumption. The SNR and BER performance of the scheme were studied in [126] and the impact of receiver's FOV was analyzed. It was discussed in [127] that the block diagonalization

algorithm for precoding results in performance uncertainty and requires the number of receiving antennas (photodiodes) to be no more than the transmitting antennas (LEDs in an array). [127] proposed to use Tomlinson-Harashima Precoding algorithm which is shown to achieve better BER performance compared to the block diagonalization algorithm.

B. Cell Design and Coordination

Cell Design: The requirement of managing access to multiple devices in VLC is different than other types of networks. This is because the size of a cell can vary depending on how illumination is provided. For example, it is possible that one multi-LED luminaire on the ceiling provides illumination to an entire room. In this case, the luminaire transmits data to multiple users each possibly with multiple devices. We refer to this type of cell as an *attocell* [128]. Based on the required illumination, it is not difficult to see that radius of an attocell is no more than 10 meters. The other type of cell is even smaller in size where the luminaire provides illumination mostly for personal usage. Such type of luminaires are commonly used to brighten small spaces in homes and spaces such as desk lamps etc. We refer to this type of cell as a *zeptocell.* The typical radius of a zeptocell is no more than 5 meters and comparatively fewer devices connect to a zeptocell.

Since multiple bright attocells are typically used for illumination of large indoor spaces, inter-cell interference is more severe for attocells. For zeptocell, each luminaire has lesser brightness compared to the luminaire of an attocell. Also, the zeptocells are deployed relatively sparsely which means that the inter-zeptocell interference is not as severe as inter-attocell interference. The cell design for outdoor scenarios is discussed in Section VI-B. In indoor spaces, a common scenario that can emerge in future is when multiple zeptocells are deployed within the range of one or more attocells. Such a heterogeneous network (referred as hetnet) is analogous to today's cellular networks where many femtocells are deployed within the range of a macrocell to meet the traffic requirement. Important problems in such hetnet scenario are managing interference between attocells and zeptocells, and determining resource-aware association bias towards the zeptocells. Also, since the primary purpose of installing luminaires is to provide illumination, it is not clear that whether the resultant cell topology is interference-optimal for the communication purpose or not. Further investigation is needed to determine interference-optimal cell topology which can maximize the throughput while meeting the illumination requirements.

In some initial efforts to design VLC cells that provide improved communication performance and also meet the illumination constraints, [130] and [129] proposed a novel LED arrangement design. It showed that SNR variation in a room is significantly high when one LED luminaire is placed at the center of the ceiling [23]. Although this is a common practice for illumination, the differences in SNR can cause serious performance degradation for the users at the edge of the room. The SNR variation is shown in Fig. 19. Authors in [130], [129] proposed to use 12 LED luminaires in a circle and 4 luminaires on the corner (with the same total emitted power) as shown in Fig. 19. It was shown that such an arrangement minimizes the variance of received power at different locations in the room. The choice of the radius of the circle of LEDs determines the delay spread of the received signal that can be optimized based on the spatial distribution of the receivers. In general, further research is necessary to design LED arrangements that can optimize communication performance while meeting the illumination constraints for a variety of indoor layouts such as homes, hospitals, shopping malls etc.

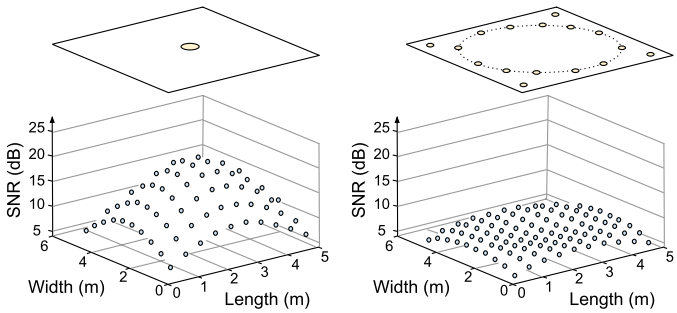

Fig. 19. Rearranging LEDs can result in lower variance of SNR in an indoor space; reproduced from [129].

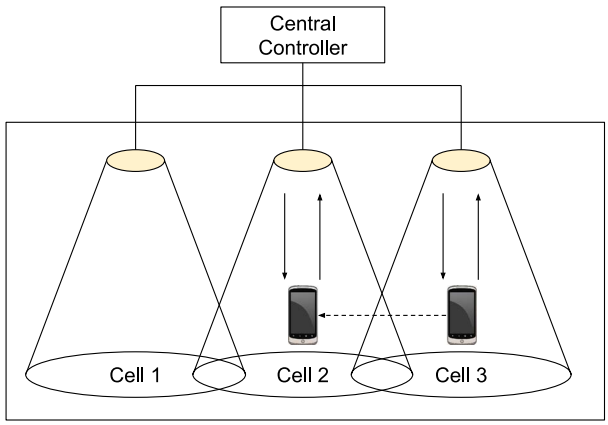

Fig. 20. Device mobility can be managed by the central controller that coordinates the operations of VLC cells; reproduced from [8].

Cell Coordination: IEEE 802.15.7 [8] provides suggestions for managing cell design and techniques to reduce inter-cell interference. It assumes that the LED transmitters in an indoor environment are connected to a central controller entity that can coordinate the cell operations and device mobility. A device associates with a cell for which the signal strength of the beacon is maximum among all the nearby cells. This is shown in Fig. 20. The mobility management framework is similar to that of WiFi or other cellular networks where a device handover occurs when the device moves from one cell to the other. For managing the inter-cell interference, the transmitters use frequency hopping where the controller ensures that interfering cells do not use the same frequency band at the same time. Note that the support of frequency hopping depends on the capabilities of the LEDs, e.g. if the LEDs are RGB LEDs, it is possible to provide many color bands that can be used for hopping. The cell management, mobility and inter-cell interference can be simplified with the use of central controller, however, it is expensive to implement

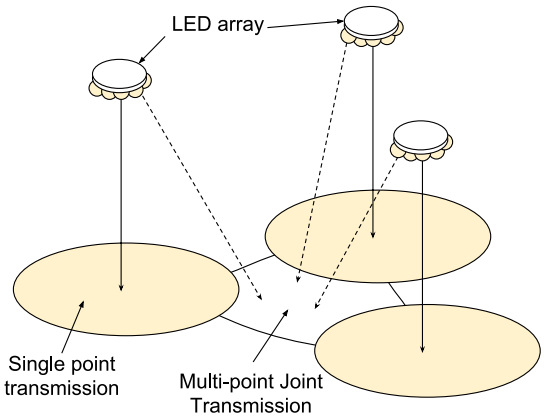

Fig. 21. Multiple LED transmitters can jointly transmit to receivers located in the multi-point joint transmission region; reproduced from [131].

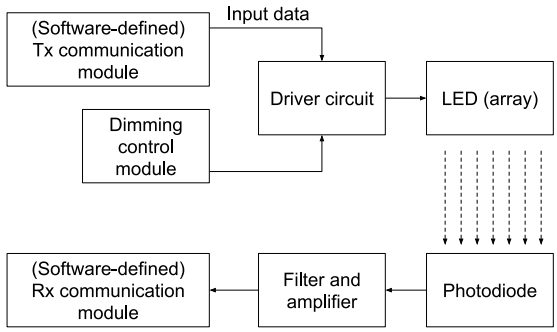

Fig. 22. A block diagram showing various modulates of VLC transmitter and receiver.

such a controller in practice due to higher deployment cost of interconnects.

Inter-cell inference is known to be a challenging problem in any type of cellular network design. From the perspective of VLC, the inter-cell interference can cause much severe degradation of SINR for the cell edge users. For example, in a room that has two LED transmitters in two parts of the room, the users in the middle of the room can experience very low SINR, which in turn results in low data rate. One of the early solution to the problem was proposed by [132] for infrared optical communication where the cells were partitioned into clusters. Different cells in a cluster used different frequency resources that are orthogonal to the neighboring cells. The frequency resources were reused between the clusters. The limitation of this approach is that bandwidth available to each individual cell is limited which reduces the achievable data rate. To improve on such static resource partitioning, authors in [133] proposed a dynamic resource allocation scheme where a channel resource is dynamically assigned to devices based on current inference. This scheme, however, incurs an overhead of additional uplink communication that is necessary to acquire a channel resource. Authors in [131] showed how multiple LEDs can transmit simultaneously to the same receiver using Joint Transmission (JT). It was shown that in order to synchronize the signals from multiple LEDs, the transmitters can use different delay values such that the signal is constructively at the receiver. The JT technique was further improved by [109] where it was shown that if the LED transmitters are made of an array of 7 LEDs each pointing to different directions, the edge users can benefit from joint transmission from LEDs of different luminaires. The joint transmission region is shown in an example in Fig. 21. Due to relatively smaller coverage of typical VLC cells, it is imperative to design interference avoidance techniques that can ensure high data rate communication even with dense deployment of receivers.

V. System Design and Reprogrammable Testbeds

In this section, we introduce the details of VLC system architecture. Detailed understanding of the system components can allow researchers to build a VLC platform that can be used to evaluate newly design protocols or techniques. We survey the existing evaluation platforms that provide *reprogrammability* and *flexibility* in VLC system design with the use of commercial off-the-shelf hardware or software-defined radio platforms.

Fig. 22 shows a schematic diagram of a VLC system with various components of the transmitter and the receiver. The transmitter communication module is responsible for modulation and digital to analog conversion of the data. The dimming module maintains the desirable dimming level for the illumination. The driver circuit combines the analog input data for communication and dimming control signal (DC power level), and superimposes them to drive the LED. The visible light signals emitted by the LED are then received by the photodiode. Note that both LED and photodiode typically employ a lens to achieve a specific FOV. The received signal is filtered using an optical filter of specific wavelength and amplified. The receiving communication module converts the received analog signals to digital and demodulates them. If the communication modules are software-defined, various modulation/demodulation and MAC modules can be programmed and evaluated. We next survey programmable VLC platforms that are used in some of the recent research.

We first discuss the low-cost solutions for VLC prototyping. We then provide how software-defined radios can be used to create VLC transceivers which provide more flexibility in design at a higher cost.

A. Low Cost VLC Prototyping Using Commodity Hardware

The objective of such VLC system design is rapid prototyping with low-cost off-the-shelf hardware.

OpenVLC is an open-source implementation for networked VLC research [134]. It consists of one BeagleBone Black (BBB) board [135] as the communication module which implements PHY and MAC layer on Linux. The OpenVLC utilizes a bidirectional front-end which can act as an LED and a photodiode as well for transmitting and receiving the light signals respectively. The transmitter and receiver mode can be switched using a tri-state buffer in the front-end circuit. In its current form, OpenVLC uses OOK modulation and Manchester RLL coding at the transmitter. At the receiver, direct detection is implemented to demodulate the OOK signals. The platform has been used for evaluation of CSMA/CD MAC protocol in [106]. Currently, OpenVLC can operate with limited wattage

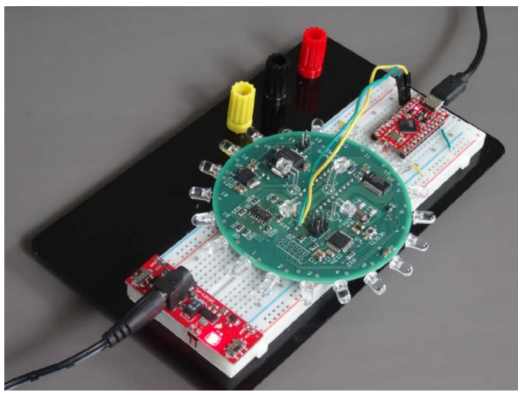

Fig. 23. VLC transmitter front-end with 20 LEDs providing 360° coverage; image from [136].

LEDs reducing its communication range to be less than a meter and throughput in range of tens of kbps.

Similar to OpenVLC, a low-cost embedded evaluation board (Atmel ATmega328P [137]) was used in the design of LED-to-LED communication in [105]. A 2-PPM based PHY and CSMA based MAC was developed to run on the embedded boards. In the testbed used in [134] and [105], the FOV of the LED is limited to the direction of LED's central axis. This limits its coverag\textbackslash e to a specific direction. This limitation was overcome by [136] where authors designed an LED front end with 20 LEDs as shown in Fig. 23. In the design, the LEDs are equally spaced to provide coverage in 360°. The advantage of such front-end is that a VLC node with multiple LEDs can communicate with multiple other nodes in different directions, enabling a multi-hop network of visible light communication nodes. The developed front-end is based on a bread-board which can interconnect with popular low-cost evaluation boards such as BeagleBone [135], Raspberry Pi [138], Arduino [139] etc.

As mentioned before, these prototyping allow faster development of VLC system at a lower cost which is sufficient in many research and commercial applications. However, their performance is often limited by the hardware (processor, ADC-DAC speeds, LED frequency etc.), which makes them more suitable for low data-rate applications. The reconfigurability of such platforms is also limited as implementation of different PHY or MAC requires significant modifications to hardware and software design.

B. VLC Prototyping With Software-Defined Radios

The use of software-defined radios allows redesigning various communication modules (PHY, MAC etc.) with much greater flexibility. They are more suitable for high data-speed applications and realistic evaluation of various PHY protocols.

Software-Defined VLC with WARP utilizes WARP platform boards [140] developed at Rice University as the software-defined communication module. The WARP platform has been used widely in RF system implementation and evaluation due to its flexibility and extensibility. A WARP-based VLC platform which was recently proposed by [141] is depicted in Fig. 24. Here, the OOK modulation and demodulation modules are

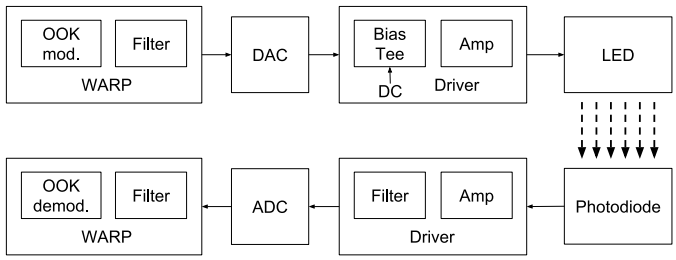

Fig. 24. Architecture of the VLC software-radio prototype; reproduced from [141].

implemented on the WARP boards. The ADC/DAC module is interfaced with the WARP board. On the transmitter side, the analog signal and the DC input are combined using a Bias Tee implemented on the driver circuit. On the receiver side, the driver circuit implements the filter and amplifier, while the ADC converts the signal to digital domain and inputs them to the WARP module. Similarly, authors of [142] demonstrated the implementation of ACO-OFDM and DCO-OFDM for VLC using the WARP boards. The WARP boards can be an ideal platform for developing a hybrid VLC-RF system as shown in [143]. With the use of different FEC codes, [141] showed to achieve a data rate of 4 mbps using OOK.

The combination of GNU Radio [144] and USRP (Universal Software Radio Platform) [145] is another popular software platform widely used for RF research. [146] developed a VLC system utilizing the USRP and GNU Radio software. BPSK, QPSK and 2048 FFT length OFDM modulation schemes were implemented in the testing, and 2 Mbps data rate was achieved in the OFDM case. Further, authors in [147] extended the VLC system by introducing an adaptive modulation for dynamic illumination that can dynamically modify the modulation schemes in order to meet both the data communications and illumination requirements of a dual-use VLC system.

The advantage of using software-defined radios is that they provide improved flexibility because various PHY and MAC modules can be implemented in software. Also, higher processing capacity of the software-defined platforms can provide high data-rates which is necessary for evaluating VLC in access network scenarios.

VI. Sensing and Other Applications

The image sensor receiver available on today's mobile devices enables a new direction of research where VLC can be combined with mobile computing to realize novel forms of sensing and applications. This sections provides an overview of such sensing and communication applications.

A. Indoor Localization

Location-based services have observed tremendous growth in last few years. Mobile device localization in outdoor scenarios largely depend on Global Positioning System (GPS). However, the GPS does not work indoors, requiring alternative ways of localizing devices. Among the alternatives, WiFi-based indoor localization has proven to be most attractive where

existing WiFi AP deployment is leveraged to identify client's location. Although low-cost, WiFi-based indoor localization offers lower accuracy (refer to [148] for overview), and complex multi-path cancellation techniques [149] are required to improve the accuracy.

Similar to WiFi-based localization, indoor visible light communication system can also be leveraged for accurate localization. The advantage of using VLC over WiFi for localization is that typically there are many more LED luminaires in a building compared to the number of WiFi APs. It was observed in [150] that there are 10 times more LED luminaires than the number of WiFi APs in a typical indoor building. This higher density can allow more accurate triangulation of the mobile device resulting in higher accuracy. Epsilon [150] presented the first practical visible light localization system. In Epsilon, the mobile device performs receiver side localization by receiving the light beacons from LED sources. Each LED source broadcasts a beacon with identity and location information. To avoid collisions between the beacons of uncoordinated LED sources, a distributed channel hopping is utilized. The receiver (a photodiode) on a mobile device receives the beacon from multiple sources. It utilizes the RSS values of received beacon to estimate the distance from the received to the LED source. Based on the distance estimates, the receiver uses trilateration to obtain its own location. Additionally, if the receiver can see less than 3 LED sources, the user can actively move the device to increase the visibility. It was shown that Epsilon can achieve the location accuracy of $\approx$0.4 meters—compared to 3–6 meters accuracy achievable in WiFi-based schemes [148].

Another practical visible light localization approach was presented in Luxapose [151]. Different from Epsilon, in Luxapose, the receiver is considered to an imaging sensor such as the smartphone camera. The user takes an image of LED luminaires using the camera. The image is then analyzed to detect the beacon information broadcast by the luminaires and the angle-of-arrival (AoA) of the beacon. Based on the orientation of the smartphone camera, angle-of-arrival from the luminaires is then used for triangulation to localize the receiver device. Luxapose to shown to achieve localization accuracy of $\approx$0.1 meters. Similar to Luxapose, it was shown in [152] how an imaging sensor can be used to receive from multiple luminaires each of which creates a visual landmark. Other variations of visible light localization include [153] where both RSS and AoA are used for two-phase hybrid localization. Authors in [154] showed that 3-D localization with sub-centimeter accuracy is also feasible using multiple tilted receivers.

With very high accuracy and ability to leverage the existing lighting infrastructure, visible light localization will on the forefront of future location-based services. Commercial products such as ByteLight [155] are already being available for retail markets.

B. Screen-Camera Communication

In this section, we take a look at a special application of VLC where an LCD screen and a camera sensor can communicate for device-to-device communication. LCD screens and cameras are widely used in today's mobile devices such as smartphones, laptops, etc. In infrastructure-to-device communication which we discussed in previous sections, LED luminaire serves a dual purpose of illumination and communication. On the other hand, screen-camera communication is a form of device-to-device communication where information can be encoded in display screens of smartphone, laptop, advertisement boards etc., and another device with a camera sensor can capture the screen and decode the data using image analysis. Due to the short wavelengths and narrow beams of visible light, LCD screen—camera links are highly directional, low-interference and secure. It was first identified in [156], [157] through analysis and experiments that such links are capable of achieving hundreds of kbps to mbps of data rates. However, there are three main challenges in such links as described in [158].

- **Perspective distortion** is a common phenomenon in daily life. When we take a look at an image on a rectangular screen from a certain angle, the image on the screen appears more like a trapezoid. In particular, we observe that some pixels shrink, while others expand. This same phenomenon is also observed in screen-camera links where some pixels have better visibility than others improving their communication reliability.
- **Blurring** occurs when the camera moves while capturing the display. The result of blurring is out-of-focus images where some pixels are blended together. In the frequency domain, blur can be considered a low-pass filter where high frequency attenuates much more than the low frequency [158].
- **Ambient light** is a source of noise which changes the luminance of the received pixels. This can cause errors in the information encoded in the pixels, resulting in information loss at the receiver. In frequency domain, since ambient light changes the overall luminance, it can be considered the DC component.

To solve these problems, inspired by traditional OFDM modulation scheme in RF, PixNet [158] proposed to encode the information in two-dimensional spatial frequencies. The main components of PixNet include a perspective correction algorithm, blur-adaptive OFDM coding and a ambient light filter. The blur-adaptive OFDM coding is introduced at the transmitter where bits are first modulated into complex numbers and then broken down to symbols, then the symbols are arranged in a two dimensional Hermitian matrix that guarantees the output is real. The transmitter treats different frequencies differently. Since the blur attenuates the high frequencies of an image, the information is transmitted through low frequency and protected with a Reed Solomon error correcting code. The RS code operates on a block size of 255 and 8 bits elements in one block. Ambient light filter at the receiver can directly filter the zero frequency caused by the ambient light. Perspective correction algorithm is partially implemented at the transmitter and partially at the receiver. It allows the PixNet system to work with an irregular Sampling Frequency Offset (SFO) caused by the perspective distortion, and use the SFO to re-sample the information at right frequencies to correctly recover the bits at the receiver.

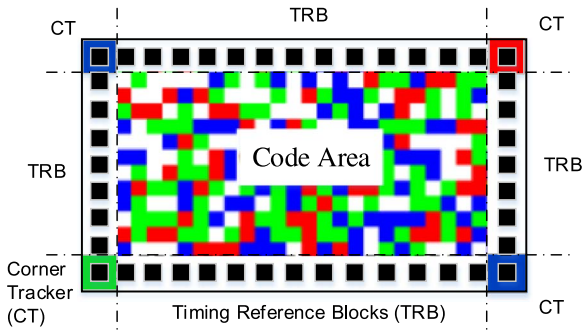

Fig. 25. Example of 2D COBRA barcode; reproduced from [159].

Another approach for screen-camera communication was presented in COlor Barcode stReaming for smArtphones (COBRA) [159]. COBRA is designed to achieve one-way communication between small size screens and low-speed cameras of smartphones using 2-D color barcodes. At the transmitter, a header and the CRC checksum are added to the original data. Then each byte of the data block is mapped to a certain color to generate a color barcode that can be displayed on the screen. The novel 2-D color barcode is shown in Fig. 25. The barcode contains three types of areas—corner trackers, timing reference blocks and code area in the center. The corner trackers are used to locate the barcode on the screen using green and red blocks at top-left and bottom-right corner respectively, and blue blocks at the other two corners. The corner trackers can then be used by the camera to detect the black and white timing reference blocks. These timing blocks are used as reference for detecting the data blocks in code area. In the code area, the data (header, payload and CRC checksum) is encoded by a sequence of color blocks in the code area. For example, assuming red, green, blue and white colors represent 00, 01, 10, and 11 respectively. In this way, a byte with value of 10110001 can be encoded as "blue white red green." At the receiver, COBRA includes a pre-processing component which selects the best quality for each barcode for further processing and a code extraction component which decodes the original information. The COBRA is successfully implemented on Android smartphone, and experimental results show that COBRA can achieve a throughput of upto 172 Kbps (much higher than PixNet's throughput of < 10 Kbps).

The limited available throughput in screen-camera links was further improved by LightSync. [160]. Authors identify that improving the frame synchronization between the transmitter and receiver can nearly double the achievable throughput. In LightSync, linear erasure coding is used to recover the lost frames and color tracking is used to decode the data correctly from imperfect frames. Another coding scheme referred as Styrofoam [161] addressed the problem of inter-symbol interference due to lack of synchronization by inserting blank frames in the code pattern. Further, authors in Hilight [162] introduced a new scheme for screen-camera communication without any coded images. Leveraging the properties of orthogonal transparency (alpha) channel, HiLight "hides" the bits by changing the pixel translucency instead of modifying the RGB color. Experimental results demonstrate the feasibility of HiLight's by using the off-the-shelf smartphones. Because screen-camera link is inherently unidirectional, [163] added reliability to the communication using tri-level error correction through packet-frame-block structure. Similarly, authors in [164] proposed variable rate screen-camera links where instead of all-or-nothing detection, various intermediate resolutions of camera can allow lower data rate (analogous to rate adaption of RF links). The proposed layered coding is shown to achieve improved reliability at larger distances with minor penalties in throughput. With increasing popularity of screen-camera links for near-field communication, it has become necessary to address the security aspects of the channel. Authors in [165] showed why is it difficult to secure the screen-camera communication, and proposed enhancements by manipulating the screen viewing angles and user motion tracking.

C. Vehicular Communication

In this section, we review the application of VLC in the vehicular communication. As the VLC based vehicular communication systems are used in the outdoor scenario, they have one distinguishing characteristic compared to the indoor applications, namely the non-negligible ambient light interference due to background solar radiation and other light sources, such as the road light, the building lights, etc. Most of the VLC vehicular communication systems address the problem and present ways to mitigate the effects of intense ambient interference.

The VLC applications for vehicular communication fall into two categories: Vehicle to Infrastructure (V2I) and Vehicle to Vehicle (V2V). For the V2I applications [166]–[168], they focus on utilizing the traffic related infrastructure, such as traffic light, street light etc. to communicate useful information. There are two types of cells in V2I communications. In the first type, the street lights whose primary purpose is to provide illumination can be used for data communication with cars or pedestrians. Such VLC cells can typically provide coverage in 50–100 meters range. The other type of outdoor LEDs are traffic signaling LEDs that can communicate with cars. Since their primary purpose is not illumination and because they are always ON (even when there is sunlight), they are more suitable for applications such as vehicle safety, traffic information broadcast etc. On the other hand, the illumination LEDs are available on streets even where there are no traffic lights, making them more suitable for high-speed Internet access type of applications. For the V2V applications [169]–[172], they mainly work on exploiting the headlights and taillights on automobile as transmitter, and the photodiode or image sensor as the receiver to provide reliable communications between vehicles.

For the VLC based vehicular communication systems, both types of receivers—the photodiode [169], [171], [172] and the image sensor [166]–[168], [173], [174] are used. Compared with the photodiode, if there are different light sources and each signal is modulated individually, the image sensor can recognize all of them simultaneously and achieve the parallel data transmission. Another advantage of the image sensor is that it is more resistant to the light interference. Since most

mobile phones have an integrated camera sensor which makes it an attractive choice for vehicular applications. However, most image sensors are limited by the *rolling shutter* scheme which means they can not capture the whole scene instantaneously but scan it vertically or horizontally. This limits the sampling rate for receiving data. On the other hand, the photodiode can support higher data rates at lower cost, which enables it as receiving devices for economic systems.

A V2I system was presented in [166] which adopts the high-speed camera deployed on the automobile to efficiently and accurately receive the signal from traffic lights. If the camera is far from LED traffic lights, it is hard to differentiate each individual data pattern sent out by the LED because of reduction of pixel size and de-focusing of the LED data pattern. Hence, the high spatial frequency components of data pattern are often lost. However, the low frequency components remain in the pixels, which means that the high-speed camera can receive the low-frequency LED data pattern contained in these pixels, even if the camera is far from the transmitter. To utilize these channel characteristics, the authors proposed a hierarchical transmission scheme which injects high priority data to low frequency components and low priority data to high frequency components to guarantee the high priority data can be received even when the camera is far away from the LED traffic lights. When the car approaches the LED traffic light, it can receive the low priority data in the low frequency components.

To enable the VLC vehicular communication (V^2LC), two primary key elements should be examined: *(i)* the feasibility of V^2LC networks in the working condition which experiences noise and interference from solar radiation and other light sources; *(ii)* the capability of V^2LC networks to provide efficient services to support vehicular applications. Liu *et al.* [169] suggested additional services feasible with V^2LC such as vehicle-to-vehicle broadcasting, infrastructure-to-vehicle broadcasting, etc. After examining the ability of V^2LC to satisfy the requirements of vehicular applications, they find V^2LC could achieve efficient communication in the dense vehicular traffic condition. V^2LC is more resilient to the background noise from solar radiation (the diffused sunlight), but is much more susceptible to the direct sunlight. Besides, the nocturnal noise coming from idle VLC transmitters as well as legacy lights with no data transmission abilities has very limited impact on V^2LC, which means V^2LC is robust to this kind of noise.

One of the most important purposes of vehicular communication systems is to provide road safety. Dedicated Short-Range Communication (DSRC, which utilizes the 5.9 GHz radio spectrum) is usually regarded as the most promising technology to support V2V communication. A comparison between DSRC and VLC was presented in [173], and following advantages of VLC over DSRC were outlined

- **Lower complexity and cost:** Due to the much smaller multipath effect, the design of VLC transmitter is much easier than the RF transmitter. Also, the LED lights already exist in auotomobiles, while RF based systems incur additional cost of deploying the equipment.
- **Scalability:** The RF based V2V communication scales poorly when the vehicle density increases in the communication range, but for VLC, only the vehicles in the LOS are in the same contention domain, which means they experience much less interference.
- **Positioning capability:** RF based positioning schemes can not provide sub-meter accuracy. The VLC provides a promising way to perform relative positioning with sub-meter accuracy due to the high directivity of visible light.
- **Security:** In the VLC scenario, if an attacker tries launch an attack, it must be within the LOS range of the victim, which means the attacker will be exposed with higher possibility. Hence, compared to the RF communication, VLC also provide a better security in vehicular communication.

With the communication and positioning capabilities of VLC, it is possible to accurately construct a map of vehicle's surrounding as shown in [171], [172]. Based on the map, a car can not only obtain the distance from other cars, but it can also broadcast its real-time speed to the neighbors through the headlight and taillight. Other vehicles receiving this information can adjust their speed accordingly (especially useful for self-driving cars) to maximize the fuel efficiency and minimize the chances of collisions.

D. Human-Computer Interaction (HCI) Using Visible Light

There is a growing interest in utilizing the wireless communication systems for enabling improved HCI. Recently, RF communication systems, especially WiFi, has been extended to perform motion detection [175], gesture recognition [176] and efficient input detection [177]. Visible light-based interaction systems are well-studied in research and many similar commercial products are available already. For example, optical mouse utilizes LEDs and photodiodes to detect fine-grained motion. Similarly, Kinect [178] system uses a combination of infrared and visible light to perform accurate 3D-gesture recognition. However, the problem with such 3D-gesture recognition systems is that they are expensive mostly because they require sophisticated image sensors along with advanced graphics techniques to process the captured images.

Some recent research has proposed inexpensive means of providing richer HCI using visible light. Authors in [179] showed that human presence or motion causes changes in the electromagnetic field around the fluorescent lamp. This changes result in variations in home/office power-line network, hence the gestures can be recognized by another pluggable module anywhere on the power-line network. Similarly, it was demonstrated in [180] how LEDs can be used to receive the visible light (like a photodiode) and applied it to different sensing applications. PICOntrol [181] showed how a pico-projector can be used to emit visible light and enable remote control to any device that has a simple embedded control unit. The projected light on the sensor unit provides a GUI where user can provide various commands to control the physical object. Okuli [182] presented a system where user's finger can be precisely

located within a small workspace using an LED and two photodiodes, allowing the user to interact with mobile/wearable devices with small form-factors. Authors in [183]–[185] designed techniques where user's gesture and complete skeleton posture can be reconstructed using her shadow (detected via photodiodes on the floor) to enable a variety of applications in smart-spaces and person identification. As LEDs become prevalent, and more and more photodiodes/image sensors are deployed in indoor environment, visible light sensing and gesture recognition have the potential to solve many contemporary HCI-related challenges.

VII. Summary and Challenges

Visible light communication has the potential to provide high speed data communication with improved energy efficiency and communication security/privacy. With looming crisis of RF spectrum shortage, VLC can become a practical augmentation technology for the existing RF networks. Increasing interest from research community and industries as well the standardization efforts such as VLCA and IEEE 802.15.7 show that VLC can be successfully commercialized in coming years.

In this survey, we provided an overview of literature covering visible light communication, networking and sensing. We first discussed various components of a visible light communication system including LED design and type of receivers. We then provided a comprehensive survey of VLC communication channel model and its propagation characteristics. This included a discussion of path loss, multi-path, SNR and shadowing. With this understanding of channel propagation, we provided a survey of VLC physical layer modulation techniques. We discussed how different modulation techniques should be able to provide dimming support and minimize flickering effect while maintaining higher spectral efficiency. This included a discussion of four major modulation techniques (OOK, PPM, OFDM and CSK). It was shown that due to their higher data rate capacity, OFDM and CSK are likely to be play an important role in future VLC broadband access networks. Additionally, feasibility of VLC MIMO as shown in literature ensures further data rate enhancements. This was followed by a survey of link layer protocols for VLC. An elaborate discussion on current CSMA, OFDMA, CDMA and MU-MIMO protocols was provided. We covered a variety of inter-cell interference management techniques, and highlighted the importance of techniques such as LED rearrangement and joint transmission. A review of existing VLC system platforms that provide reprogrammability and flexibility of implementation was then provided with a discussion on low-cost platforms as well as software-defined platforms. We then provided a detailed survey of an interesting upcoming field of VLC sensing where literature on visible light localization, screen-camera NFC, vehicular networking and VLC-assisted HCI techniques was reviewed.

Based on the review of current literature on VLC, we now outline the important challenges that need to be addressed in near future. Solving these challenges are essential so that VLC can be deployed in practice as a high-speed mobile networking technology.

A. FOV Alignment and Shadowing

The techniques of achieving high data rates in VLC links primarily assume an LOS channel where the transmitter and the receiver have aligned their field of views to maximize the channel response. However, in more practical scenarios, receiver movement and orientation changes are common. For example, in VLC-based indoor access network, user's smartphone equipped with a light sensor can move and rotate based on user's actions. This means that receiver's FOV cannot always be aligned with the transmitter. As we saw in Section III-A, the drop in received optical power can be significant due to such misalignment. It is necessary to design techniques that can ensure high data rates even in the presence of FOV misalignment cases. This requires design and development of methods that can provide graceful degradation in data rate using the optical power of reflected light. Designing such techniques is extremely challenging and is an important direction of future research.

Apart from the FOV alignment, another critical limitation is imposed by shadowing events. When an object or human blocks the LOS, the observed optical power degrades substantially, resulting in severe data rate reduction. As discussed in Section III-A5, limited research is done to understand/model the effect of shadowing events on VLC. When the LOS is blocked by a shadowing event, it is not only necessary to exploit the reflected optical power of the diffuse channels but it also necessary to do so in a timely manner as typical blockage events can be of very short duration (e.g. human passing by). Thus, it is imperative to design techniques that can quickly react to changes in received power due to FOV misalignment and shadowing.

B. Receiver Design and Energy Efficiency

Current VLC receivers either use a photodiode or an imaging sensor for receiving the VLC signals. The use of photodiode is more suitable for stationary clients where its FOV can be aligned to the LED fixture for high received optical power. On the mobile devices, the imaging sensor can be used since they have comparatively larger FOV (due to wider concentration lens), making the mobile device a little more robust to movements and FOV misalignment. However, due to a large number of photodiodes, operating imaging sensor is slow and energy expensive. This can significantly slow down the overall achievable data rate. This is natural given that imaging sensor was primarily designed for image and video capture, and not for the communication. Thus, it is challenging to design a receiver that can provide robustness to device movements and FOV misalignment. The receiver should also operate with low energy consumption to be useful on battery-powered mobile devices while providing high-speed visible light communication.

C. LED to Internet Connectivity

In order to create a VLC-based broadband access network, it is necessary to connect the LEDs to Internet. Because the deployment of LEDs (for illumination purposes) is likely to be very dense, it becomes a challenging problem to connect

the large number of LEDs to Internet. The cost of deploying wired infrastructure (e.g. Ethernet, fiber etc.) can be very high, which in turn can cancel the benefits of reusing the LEDs for communication. Providing wireless connectivity is feasible, however, with dense deployment of LEDs, the interference of wireless connections can be a limiting factor. This can reduce the achievable Internet data rate for the LEDs. In some recent work, power-line communication has been proposed in [186] as a way to interconnect LEDs. The power-line communication provides an attractive choice as it can reuse the existing power line network for communication without additional cost of cable deployment. However, the use of power line incurs cost overheads of using Ethernet-to-power modem and power-to VLC modems. Apart from this cost, the performance and coverage issues [187] of power line communications should be addressed for successful power-line and VLC integration. There is a scope for designing novel techniques that can provide high-speed Internet connectivity to the LEDs at low cost.

D. Inter-Cell Interference

The dense deployments of LEDs can provide higher capacity due to smaller cell radius. However, as discussed in Section IV-B, the VLC small cell architecture puts forward a challenge of managing inter-cell interference. On one hand, visible light communication provides less interference since the visible light is blocked by walls which naturally restricts its propagation to rooms in indoor spaces. On the other hand, the LEDs inside a room (in the same collision domain) can cause severe interference to each other, and the performance can degrade due to low SINR. The problem can be solved by employing various techniques such as network MIMO, joint transmission and LED rearrangement. In network MIMO and joint transmission, the interfering LEDs can coordinate their transmissions via interference nulling or synchronization to ensure high SINR at the receivers. Another method to combat the interference is to rearrange the LEDs such that their mutual interference is less. For this method, systematic design and analysis are required for optimizing the communication performance while meeting the illumination constraints.

E. Uplink and RF Augmentation

Almost all current research in visible light networking focuses on downlink (from LED luminaire to photodiode/image sensor receiver) traffic without taking into consideration how the uplink can operate. Although efficient LEDs are incorporated in today's mobile devices as camera flashlight or notification indicator, they can not be used directly for communication. This is because constantly turning on the LED not only consumes significant energy for mobile devices but it also causes visual disturbance to users while using the devices. Also, VLC uplink requires that user's mobile device maintains a directional beam towards the receiver which can result in significant throughput reductions when the mobile device is constantly moving/rotating. To address these challenges, use of other types of communication has been proposed where RF [188]–[190] or infrared [191] can be used for transmitting uplink data.

RF-based uplink transmission is an attractive alternative considering that WiFi is already omni-present especially in indoor environments. Operating VLC small cells under the coverage of WiFi cells (larger range) also ensures that clients have uninterrupted connectivity when VLC communication is not available (e.g. night time, blockage etc.) Utilizing 3G and 4G cellular networks such as LTE is also feasible, however, they impose additional challenges when the indoor wireless network provider is different than the cellular network provider. Utilizing different communication technologies for uplink and downlink gives rise to heterogeneous networks (HetNets) [192]–[194]. Such networks impose additional practical challenges such as complex network management for multi-homed clients [195], throughput asymmetry issues for transport layer [196], link-layer packet loss management and reliable data delivery etc. There is only a limited amount of research done in asymmetric and heterogeneous networking. In order to build robust high-speed HetNet of VLC and RF, it is crucial that these challenges are resolved.

F. Mobility and Coverage

In order for VLC to be a ubiquitous mobile technology, it is necessary that it can provide uninterrupted and high-speed connectivity in presence of user mobility within a VLC cell and between the VLC cells. User mobility introduces novel issues for VLC that are significantly different than RF. For example, as shown in [141], even in a small VLC cell, the client SNR varies dramatically (many times within the frame transmission duration) when user moves within the cell. These fast variations have to be accounted for when designing various link-layer techniques such as rate adaptation, frame aggregation etc. In many indoor places, LED deployment is intentionally made sparser to leverage the existing sunlight. When using LEDs for communication, it is necessary that sufficient coverage is available in all areas of an indoor space. When VLC is used as augmentation to RF networks, user mobility requires seamlessly managing horizontal (VLC to VLC) as well as vertical (VLC to RF) handover of user devices.

Apart from these challenges, some recent research [197] has shown the feasibility of eavesdropping on visible light communication from outside a room using the light signals leaked through the gap between floor and door, keyhole and even partially covered windows. These early insights demonstrate that further investigations are required to evaluate security/privacy of VLC in access networks. The challenges described above primarily stem from the use of mobile devices as receivers. To successfully build and operate a VLC access network, it is imperative to address the issues such as device movement, user mobility and energy efficiency in the design. Most of the current research in VLC has focused on physical and MAC layer performance enhancements with stationary devices. Equipped with these techniques, one of the most important direction of future research in VLC is the urgent need to address the issues that arise when utilizing mobile devices in VLC access networks. As discussed before, researchers have already started addressing these challenges, and more and more research is likely to follow the direction in near future.

REFERENCES

[1] United States Department of Energy. Energy Savings Forecast of Solid-State Lighting in General Illumination Applications. [Online]. Available: http://apps1.eere.energy.gov/buildings/publications/pdfs/ssl/energysavingsforecast14.pdf

[2] Y. Tanaka, S. Haruyama, and M. Nakagawa, "Wireless optical transmissions with white colored LED for wireless home links," in *Proc. 11th IEEE Int. Symp. PIMRC*, 2000, vol. 2, pp. 1325–1329.

[3] Visible Light Communications Consortium (VLCC). [Online]. Available: http://www.vlcc.net/

[4] Japan Electronics and Information Technology Industries Association (JEITA). [Online]. Available: http://www.jeita.or.jp/

[5] Infrared Data Association (IrDA). [Online]. Available: http://www.irda.org

[6] Home Gigabit Access (OMEGA) Project. [Online]. Available: http://www.ict-omega.eu/

[7] Visible Light Communications Association (VLCA). [Online]. Available: http://vlca.net/

[8] *IEEE Standard for Local and Metropolitan Area Networks-Part 15.7: Short-Range Wireless Optical Communication Using Visible Light*, IEEE Std. 802.15.7, Sep. 2011.

[9] D. Karunatilaka, F. Zafar, V. Kalavally, and R. Parthiban, "LED based indoor visible light communications: State of the art," *IEEE Commun. Surveys Tuts.*, vol. 17, no. 3, pp. 1649–1678, 3rd Quart. 2015.

[10] D. Tsonev, S. Videv, and H. Haas, "Light fidelity (Li-Fi): Towards all-optical networking," in *Proc. SPIE OPTO*. 2013, Art ID. 900702.

[11] A. Sevincer, A. Bhattarai, M. Bilgi, M. Yuksel, and N. Pala, "LIGHTNETs: Smart LIGHTing and mobile optical wireless NETworks—A survey," *IEEE Commun. Surveys Tuts.*, vol. 15, no. 4, pp. 1620–1641, 4th Quart. 2013.

[12] M. Khalighi and M. Uysal, "Survey on free space optical communication: A communication theory perspective," *IEEE Commun. Surveys Tuts.*, vol. 16, no. 4, pp. 2231–2258, 4th Quart. 2014.

[13] F. Demers, H. Yanikomeroglu, and M. St-Hilaire, "A survey of opportunities for free space optics in next generation cellular networks," in *Proc. 9th CNSR*, May 2011, pp. 210–216.

[14] N. Kumar and N. R. Lourenco, "LED-based visible light communication system: A brief survey and investigation," *J. Eng. Appl. Sci.*, vol. 5, no. 4, pp. 296–307, 2010.

[15] Deviant Art. [Online]. Available: http://flexpoint.deviantart.com/art/Small-Living-Room-87530751

[16] C. Danakis, M. Afgani, G. Povey, I. Underwood, and H. Haas, "Using a CMOS camera sensor for visible light communication," in *Proc. IEEE GC Wkshps*, Dec. 2012, pp. 1244–1248.

[17] A. Zukauskas, M. Shur, and R. Gaska, *Introduction to Solid-State Lighting*. Hoboken, NJ, USA: Wiley, 2002.

[18] CIE, *Commission Internationale de lEclairage Proc*. Cambridge, U.K.: Cambridge Univ. Press, 1931.

[19] Cree XLamp XP-E High-Efficiency White. [Online]. Available: http://www.cree.com/~/media/Files/Cree/LED Components and Modules/XLamp/Data and Binning/XLampXPEHEW.pdf

[20] G. Wyszecki and W. Stiles, *Color Science: Concepts and Methods, Quantitative Data and Formulae*. Hoboken, NJ, USA: Wiley, Aug. 2000.

[21] Cree XLAMP XR-E. [Online]. Available: http://www.cree.com/~/media/Files/Cree/LED Components and Modules/XLamp/Data and Binning/XLamp7090XRE.pdf

[22] Cree LMH6. [Online]. Available: http://www.cree.com/~/media/Files/Cree/LED Components and Modules/Modules/Data sheets/LEDModules_LMH6.pdf

[23] T. Komine and M. Nakagawa, "Fundamental analysis for visible-light communication system using LED lights," *IEEE Trans. Consum. Electron.*, vol. 50, no. 1, pp. 100–107, Feb. 2004.

[24] K. Cui, G. Chen, Z. Xu, and R. Roberts, "Line-of-sight visible light communication system design and demonstration," in *Proc. 7th Int. Symp. CSNDSP*, Jul. 2010, pp. 621–625.

[25] Spectral Response of a Photodiode. [Online]. Available: http://en.wikipedia.org/wiki/Photodiode

[26] B. Xie *et al.*, "LIPS: A light intensity based positioning system for indoor environments," *arXiv preprint arXiv:1403.2331*, 2014.

[27] K. Lee, H. Park, and J. Barry, "Indoor channel characteristics for visible light communications," *IEEE Commun. Lett.*, vol. 15, no. 2, pp. 217–219, Feb. 2011.

[28] K. Cui, "Physical layer characteristics and techniques for visible light communications," Ph.D. dissertation, Dept. Elect. Comput. Eng., Univ. California, Riverside, CA, USA, 2012.

[29] S. Lee, J. K. Kwon, S.-Y. Jung, and Y.-H. Kwon, "Evaluation of visible light communication channel delay profiles for automotive applications," *EURASIP J. Wireless Commun. Netw.*, vol. 2012, pp. 1–8, 2012.

[30] L. Yuan-jian, S. Qin-jian, M. Xue, and Z. Ye-rong, "Simulation and analysis of indoor visible light propagation characteristics based on the method of SBR/image," *Int. J. Antennas Propag.*, vol. 2014, 2014, Art ID. 905916.

[31] Z. Ghassemlooy, W. Popoola, and S. Rajbhandari, *Optical Wireless Communications: System and Channel Modelling With MATLAB*, 1st ed. Boca Raton, FL, USA: CRC Press, 2012.

[32] T. Komine and M. Nakagawa, "A study of shadowing on indoor visible-light wireless communication utilizing plural white LED lightings," in *Proc. 1st Int. Symp. Wireless Commun. Syst.*, Sep. 2004, pp. 36–40.

[33] M. S. Rea, *The IESNA Lighting Handbook: Reference & Application*. New York, NY, USA: Illuminating Eng. Soc. North America, 2000.

[34] S. M. Berman, D. S. Greehouse, I. L. Bailey, R. D. Clear, and T. W. Raasch, "Human electroretinogram responses to video displays, fluorescent lighting, and other high frequency sources," *Optom. Vis. Sci.*, vol. 68, no. 8, pp. 645–662, Aug. 1991.

[35] J. Grubor, S. C. J. Lee, K.-D. Langer, T. Koonen, and J. W. Walewski, "Wireless high-speed data transmission with phosphorescent white-light LEDs," in *Proc. 33rd Eur. Conf. Exhib. Opt. Commun.—Post-Deadline Papers (published 2008)*, Sep. 2007, pp. 1–2.

[36] S. Park *et al.*, "Information broadcasting system based on visible light signboard," *Proc. Wireless Opt. Commun.*, 2007, pp. 311–313.

[37] H. L. Minh *et al.*, "High-speed visible light communications using multiple-resonant equalization," *IEEE Photon. Technol. Lett.*, vol. 20, no. 14, pp. 1243–1245, Jul. 2008.

[38] J. Vucic *et al.*, "125 Mbit/s over 5 m wireless distance by use of OOK-Modulated phosphorescent white LEDs," in *Proc. 35th ECOC*, Sep. 2009, pp. 1–2.

[39] J. Vucic *et al.*, "230 Mbit/s via a wireless visible-light link based on OOK modulation of phosphorescent white LEDs," in *Proc. Conf. OFC/NFOEC*, Mar. 2010, pp. 1–3.

[40] N. Fujimoto and H. Mochizuki, "477 Mbit/s visible light transmission based on OOK-NRZ modulation using a single commercially available visible LED and a practical LED driver with a pre-emphasis circuit," presented at the Optical Fiber Communication Conf./Nat. Fiber Optic Engineers Conf., Anaheim, CA, USA, Mar. 17–21, 2013, Paper JTh2A.73.

[41] S. Muthu and J. Gaines, "Red, green and blue LED-based white light source: Implementation challenges and control design," in *Conf. Rec. IEEE 38th IAS Annu. Meeting*, Oct 2003, vol. 1, pp. 515–522.

[42] S. Kaur, W. Liu, and D. Castor, VLC dimming support IEEE 802.15-09-0641-00-0007. [Online]. Available: https://mentor.ieee.org/802.15/dcn/09/15-09-0641-00-0007-vlc-dimming-proposal.pdf

[43] J. K. Kwon, "Inverse source coding for dimming in visible light communications using NRZ-OOK on reliable links," *IEEE Photon. Technol. Lett.*, vol. 22, no. 19, pp. 1455–1457, Oct. 2010.

[44] G. Ntogari, T. Kamalakis, J. Walewski, and T. Sphicopoulos, "Combining illumination dimming based on pulse-width modulation with visible-light communications based on discrete multitone," *IEEE/OSA J. Opt. Commun. Netw.*, vol. 3, no. 1, pp. 56–65, Jan. 2011.

[45] H. Sugiyama, S. Haruyama, and M. Nakagawa, "Brightness control methods for illumination and visible-light communication systems," in *Proc. 3rd ICWMC*, Mar. 2007, p. 78.

[46] J. Vucic, C. Kottke, S. Nerreter, K.-D. Langer, and J. Walewski, "513 Mbit/s visible light communications link based on DMT-modulation of a white LED," *J. Lightw. Technol.*, vol. 28, no. 24, pp. 3512–3518, Dec. 2010.

[47] C. Georghiades, "Modulation and coding for throughput-efficient optical systems," *IEEE Trans. Inf. Theory*, vol. 40, no. 5, pp. 1313–1326, Sep. 1994.

[48] D. shan Shiu and J. Kahn, "Differential pulse-position modulation for power-efficient optical communication," *IEEE Trans. Commun.*, vol. 47, no. 8, pp. 1201–1210, Aug. 1999.

[49] F. Gfeller, W. Hirt, M. de Lange, and B. Weiss, "Wireless infrared transmission: How to reach all office space," in *Proc. IEEE 46th Veh. Technol. Conf., Mobile Technol. Hum. Race*, Apr 1996, vol. 3, pp. 1535–1539.

[50] T. Ohtsuki, "Rate adaptive transmission scheme using punctured convolutional codes in a fixed channel reuse strategy with PPM CDMA," in *Proc. GLOBECOM, Bridge Global Integr.*, 1998, vol. 1, pp. 207–212.

[51] T. Ohtsuki, "Rate-adaptive indoor infrared wireless communication systems using repeated and punctured convolutional codes," vol. 4, no. 2, pp. 56–58, Feb. 2000.

[52] B. Bai, Z. Xu, and Y. Fan, "Joint LED dimming and high capacity visible light communication by overlapping PPM," in *Proc. 19th Annu. WOCC*, May 2010, pp. 1–5.

[53] H. Sugiyama and K. Nosu, "MPPM: A method for improving the band-utilization efficiency in optical PPM," *J. Lightw. Technol.*, vol. 7, no. 3, pp. 465–472, Mar. 1989.

[54] T. Ohtsuki, I. Sasase, and S. Mori, "Overlapping multi-pulse pulse position modulation in optical direct detection channel," in *Techn. Program, Conf. Rec. IEEE ICC*, May 1993, vol. 2, pp. 1123–1127.

[55] T. Ohtsuki, I. Sasase, and S. Mori, "Performance analysis of overlapping multi-pulse pulse position modulation (OMPPM) in noisy photon counting channel," in *Proc. IEEE Int. Symp. Inf. Theory*, Jun. 1994, p. 80.

[56] T. Ohtsuki and I. Sasase, "Capacity and cutoff rate of overlapping multi-pulse pulse position modulation (OMPPM) in optical direct-detection channel: Quantum-limited case," *IEICE Trans. Fundam. Electron., Commun. Comput. Sci.*, vol. 77, no. 8, pp. 1298–1308, 1994.

[57] T. Ohtsuki, I. Sasase, and S. Mori, "Trellis coded overlapping multi-pulse pulse position modulation in optical direct detection channel," in *Proc. IEEE SUPERCOMM/ICC, Conf. Rec.*, May 1994, vol. 2, pp. 675–679.

[58] T. Ohtsuki and I. Sasase, "Error performance of overlapping multi-pulse pulse position modulation (OMPPM) and trellis coded OMPPM in optical direct-detection channel," *IEICE Trans. Commun.*, vol. 77, no. 9, pp. 1133–1143, 1994.

[59] D. Zwillinger, "Differential PPM has a higher throughput than PPM for the band-limited and average-power-limited optical channel," *IEEE Trans. Inf. Theory*, vol. 34, no. 5, pp. 1269–1273, Sep. 1988.

[60] T. Ohtsuki, I. Sasase, and S. Mori, "Differential overlapping pulse position modulation in optical direct-detection channel," in *IEEE SUPERCOMM/ICC, Conf. Rec.*, May 1994, vol. 2, pp. 680–684.

[61] M. Noshad and M. Brandt-Pearce, "Expurgated PPM using symmetric balanced incomplete block designs," *IEEE Commun. Lett.*, vol. 16, no. 7, pp. 968–971, Jul. 2012.

[62] M. Noshad and M. Brandt-Pearce, "Application of expurgated PPM to indoor visible light communications; Part I: Single-user systems," *J. Lightwave Technol.*, vol. 32, no. 5, pp. 875–882, Mar. 2014.

[63] M. Noshad and M. Brandt-Pearce, "Multilevel pulse-position modulation based on balanced incomplete block designs," in *Proc. IEEE GLOBECOM*, Dec. 2012, pp. 2930–2935.

[64] M. Afgani, H. Haas, H. Elgala, and D. Knipp, "Visible light communication using OFDM," in *Proc. 2nd Int. Conf. TRIDENTCOM*, 2006, pp. 129 pp.–134.

[65] J. Armstrong and A. Lowery, "Power efficient optical OFDM," *Electron. Lett.*, vol. 42, no. 6, pp. 370–372, Mar. 2006.

[66] H. Elgala, R. Mesleh, H. Haas, and B. Pricope, "OFDM visible light wireless communication based on white LEDs," in *Proc. IEEE 65th VTC-Spring*, Apr. 2007, pp. 2185–2189.

[67] Y. Tanaka, T. Komine, S. Haruyama, and M. Nakagawa, "Indoor visible light data transmission system utilizing white LED lights," *IEICE Trans. Commun.*, vol. 86, no. 8, pp. 2440–2454, 2003.

[68] R. Mesleh, H. Elgala, and H. Haas, "Performance analysis of indoor OFDM optical wireless communication systems," in *Proc. IEEE WCNC*, Apr. 2012, pp. 1005–1010.

[69] H. Burchardt, N. Serafimovski, D. Tsonev, S. Videv, and H. Haas, "VLC: Beyond point-to-point communication," *IEEE Commun. Mag.*, vol. 52, no. 7, pp. 98–105, Jul. 2014.

[70] H. Elgala, R. Mesleh, and H. Haas, "A study of LED nonlinearity effects on optical wireless transmission using OFDM," in *Proc. IFIP Int. Conf. WOCN*, Apr. 2009, pp. 1–5.

[71] H. Elgala, R. Mesleh, and H. Haas, "Practical considerations for indoor wireless optical system implementation using OFDM," in *Proc. 10th ConTEL*, Jun. 2009, pp. 25–29.

[72] Z. Wang, C. Yu, W.-D. Zhong, J. Chen, and W. Chen, "Performance of variable M-QAM OFDM visible light communication system with dimming control," in *Proc. 17th OECC*, Jul. 2012, pp. 741–742.

[73] A. Khalid, G. Cossu, R. Corsini, P. Choudhury, and E. Ciaramella, "1-Gb/s transmission over a phosphorescent white LED by using rate-adaptive discrete multitone modulation," *IEEE Photon. J.*, vol. 4, no. 5, pp. 1465–1473, Oct. 2012.

[74] D. Tsonev *et al.*, "A 3-Gb/s single-LED OFDM-based wireless VLC link using a gallium nitride LED," *IEEE Photon. Technol. Lett.*, vol. 26, no. 7, pp. 637–640, Apr. 2014.

[75] R. Drost and B. Sadler, "Constellation design for color-shift keying using billiards algorithms," in *Proc. 2010 IEEE GC Wkshps*, Dec. 2010, pp. 980–984.

[76] E. Monteiro and S. Hranilovic, "Constellation design for color-shift keying using interior point methods," in *Proc. IEEE GC Wkshps*, Dec. 2012, pp. 1224–1228.

[77] E. Monteiro and S. Hranilovic, "Design and implementation of color-shift keying for visible light communications," *J. Lightw. Technol.*, vol. 32, no. 10, pp. 2053–2060, May 2014.

[78] R. Singh, T. O'Farrell, and J. David, "An enhanced color shift keying modulation scheme for high-speed wireless visible light communications," *J. Lightw. Technol.*, vol. 32, no. 14, pp. 2582–2592, Jul. 2014.

[79] S. Rajagopal, R. Roberts, and S.-K. Lim, "IEEE 802.15.7 visible light communication: Modulation schemes and dimming support," *IEEE Commun. Mag.*, vol. 50, no. 3, pp. 72–82, Mar. 2012.

[80] A. Yokoi, J. Son, and T. Bae, CSK constellation in all color band combinations. [Online]. Available: http://mentor.ieee.org/802.15/dcn/11/15-11-0247-00-0007-csk-constellation-in-all-color-bandcombinations.pdf

[81] CIE 1931 Chromaticity diagram. [Online]. Available: http://commons.wikimedia.org/wiki/File:Cie_chromaticity_diagram_wavelength.png

[82] J. Vucic, C. Kottke, K. Habel, and K.-D. Langer, "803 Mbit/s visible light WDM link based on DMT modulation of a single RGB LED luminary," in *Proc. OFC/NFOEC*, Mar. 2011, pp. 1–3.

[83] F.-M. Wu *et al.*, "3.22-Gb/s WDM visible light communication of a single RGB LED employing carrier-less amplitude and phase modulation," presented at the Optical Fiber Communication Conf./Nat. Fiber Optic Engineering Conf., Anaheim, CA, USA, Mar. 17–21, 2013, Paper OTh1G.4.

[84] L. Zeng *et al.*, "High data rate multiple input multiple output (MIMO) optical wireless communications using white led lighting," *IEEE J. Sel. Areas Commun.*, vol. 27, no. 9, pp. 1654–1662, Dec. 2009.

[85] D. O'Brien, "Multi-Input Multi-Output (MIMO) indoor optical wireless communications," in *Conf. Rec. 43rd Asilomar Conf. Signals, Syst. Comput.*, Nov. 2009, pp. 1636–1639.

[86] D. Tsonev, S. Sinanovic, and H. Haas, "Practical MIMO capacity for indoor optical wireless communication with white LEDs," in *Proc. IEEE 77th VTC Spring*, Jun. 2013, pp. 1–5.

[87] J. C. Chau and T. D. Little, "Scalable imaging VLC receivers with token-based pixel selection for spatial multiplexing," in *Proc. 1st ACM MobiCom Workshop Visible Light Commun. Syst.*, 2014, pp. 21–26.

[88] T. Fath and H. Haas, "Performance comparison of MIMO techniques for optical wireless communications in indoor environments," *IEEE Trans. Commun.*, vol. 61, no. 2, pp. 733–742, Feb. 2013.

[89] D. Takase and T. Ohtsuki, "Optical wireless MIMO communications (OMIMO)," in *Proc. IEEE GLOBECOM*, Nov 2004, vol. 2, pp. 928–932.

[90] D. Takase and T. Ohtsuki, "Performance analysis of optical wireless MIMO with optical beat interference," in *Proc. 2005 IEEE ICC*, May 2005, vol. 2, pp. 954–958.

[91] D. Takase and T. Ohtsuki, "Spatial multiplexing in optical wireless MIMO communications over indoor environment," *IEICE Trans. Commun.*, vol. 89, no. 4, pp. 1364–1371, 2006.

[92] Y. Chau and S.-H. Yu, "Space modulation on wireless fading channels," in *Proc. IEEE VTS 54th VTC Fall.* , 2001, vol. 3, pp. 1668–1671.

[93] R. Mesleh, H. Elgala, and H. Haas, "Optical spatial modulation," *IEEE/OSA J. Opt. Commun. Netw.*, vol. 3, no. 3, pp. 234–244, Mar. 2011.

[94] C. Vladeanu, "Turbo trellis-coded spatial modulation," in *Proc. IEEE GLOBECOM*, Dec. 2012, pp. 4024–4029.

[95] T. Fath, H. Haas, M. Di Renzo, and R. Mesleh, "Spatial modulation applied to optical wireless communications in indoor LOS environments," in *Proc. IEEE GLOBECOM*, Dec. 2011, pp. 1–5.

[96] P. Butala, H. Elgala, and T. Little, "Performance of optical spatial modulation and spatial multiplexing with imaging receiver," in *Proc. IEEE WCNC*, Apr. 2014, pp. 394–399.

[97] T. Fath, M. Di Renzo, and H. Haas, "On the performance of space shift keying for optical wireless communications," in *Proc. IEEE GC Wkshps.*, Dec. 2010, pp. 990–994.

[98] M. Di Renzo and H. Haas, "On the performance of Space Shift Keying MIMO systems over correlated Rician fading channels," in *Proc. Int. ITG WSA*, Feb. 2010, pp. 72–79.

[99] S. Videv and H. Haas, "Practical space shift keying VLC system," in *Proc. IEEE WCNC*, Apr. 2014, pp. 405–409.

[100] M. Di Renzo and H. Haas, "Space shift keying (SSK) modulation with partial channel state information: Optimal detector and performance analysis over fading channels," *IEEE Trans. Commun.*, vol. 58, no. 11, pp. 3196–3210, Nov. 2010.

[101] W. Popoola, E. Poves, and H. Haas, "Generalised space shift keying for visible light communications," in *Proc. 8th Int. Symp. CSNDSP*, Jul. 2012, pp. 1–4.

[102] D. Takase and T. Ohtsuki, "Optical wireless MIMO (OMIMO) with backward spatial filter (BSF) in diffuse channels," in *Proc. IEEE ICC*, Jun. 2007, pp. 2462–2467.

[103] S.-M. Kim and S.-M. Kim, "Performance improvement of visible light communications using optical beamforming," in *Proc. 5th ICUFN*, Jul. 2013, pp. 362–365.

[104] L. Wu, Z. Zhang, and H. Liu, "Transmit beamforming for MIMO optical wireless communication systems," *Wireless Pers. Commun.*, vol. 78, no. 1, pp. 615–628, Sep. 2014.

[105] S. Schmid, G. Corbellini, S. Mangold, and T. R. Gross, "LED-to-LED visible light communication networks," in *Proc. 14th ACM Int. Symp. MobiHoc*, 2013, pp. 1–10.

[106] Q. Wang and D. Giustiniano, "Communication networks of visible light emitting diodes with intra-frame bidirectional transmission," in *Proc. 10th ACM CoNEXT*, 2014, pp. 21–28.

[107] J. Dang and Z. Zhang, "Comparison of optical OFDM-IDMA and optical OFDMA for uplink visible light communications," in *Proc. Int. Conf. WCSP*, Oct. 2012, pp. 1–6.

[108] D. Bykhovsky and S. Arnon, "Multiple access resource allocation in visible light communication systems," *J. Lightw. Technol.*, vol. 32, no. 8, pp. 1594–1600, Apr. 2014.

[109] C. Chen, D. Tsonev, and H. Haas, "Joint transmission in indoor visible light communication downlink cellular networks," in *Proc. 2013 IEEE GC Wkshps*, Dec. 2013, pp. 1127–1132.

[110] J. Salehi, "Code division multiple-access techniques in optical fiber networks. I. Fundamental principles," *IEEE Trans. Commun.*, vol. 37, no. 8, pp. 824–833, Aug. 1989.

[111] J. Salehi and C. Brackett, "Code division multiple-access techniques in optical fiber networks. II. Systems performance analysis," *IEEE Trans. Commun.*, vol. 37, no. 8, pp. 834–842, Aug. 1989.

[112] M. Guerra-Medina *et al.*, "Ethernet-OCDMA system for multi-user visible light communications," *Electron. Lett.*, vol. 48, no. 4, pp. 227–228, Feb. 2012.

[113] P. Kumar, R. Omrani, J. Touch, A. Willner, and P. Saghari, "A novel optical CDMA modulation scheme: Code cycle modulation," in *Proc. IEEE GLOBECOM*, Nov. 2006, pp. 1–5.

[114] M. Noshad and M. Brandt-Pearce, "Application of expurgated PPM to indoor visible light communications—Part II: Access networks," *J. Lightw. Technol.*, vol. 32, no. 5, pp. 883–890, Mar. 2014.

[115] M. Noshad and M. Brandt-Pearce, "High-speed visible light indoor networks based on optical orthogonal codes and combinatorial designs," in *Proc. IEEE GLOBECOM*, Dec. 2013, pp. 2436–2441.

[116] J. Martin-Gonzalez, E. Poves, and F. Lopez-Hernandez, "Random optical codes used in optical networks," *IET Commun.*, vol. 3, no. 8, pp. 1392–1401, Aug. 2009.

[117] M. Guerra-Medina, B. Rojas-Guillama, O. Gonzalez, J. Martin-Gonzalez, E. Poves, and F. Lopez-Hernandez, "Experimental optical code-division multiple access system for visible light communications," in *Proc. WTS*, Apr. 2011, pp. 1–6.

[118] J. Liu, Z. Pan, W. Noonpakdee, and S. Shimamoto, "Impact of light reflection on indoor wireless optical CDMA systems," *IEEE/OSA J. Opt. Commun. Netw.*, vol. 4, no. 12, pp. 989–996, Dec. 2012.

[119] J. Lian, M. Noshad, and M. Brandt-Pearce, "Multiuser MISO indoor visible light communications," in *Proc. 48th Asilomar Conf. Signals, Syst. Comput.*, Nov. 2014, pp. 1729–1733.

[120] S.-H. Chen and C.-W. Chow, "Color-shift keying and code-division multiple-access transmission for RGB-LED visible light communications using mobile phone camera," *IEEE Photon. J.*, vol. 6, no. 6, pp. 1–6, Dec. 2014.

[121] J. Luna-Rivera *et al.*, "Multiuser scheme for indoor visible light communications using RGB LEDs," in *Proc. IWOBI*, Jul. 2014, pp. 119–123.

[122] C. Yang, Y. Wang, Y. Wang, X. Huang, and N. Chi, "Demonstration of high-speed multi-user multi-carrier CDMA visible light communication," *Opt. Commun.*, vol. 336, pp. 269–272, 2015.

[123] L. L. Hanzo, M. Münster, B. Choi, and T. Keller, *OFDM and MC-CDMA for Broadband Multi-User Communications, WLANs and Broadcasting*. Hoboken, NJ, USA: Wiley, 2005.

[124] Z. Yu, R. Baxley, and G. Zhou, "Multi-user MISO broadcasting for indoor visible light communication," in *Proc. IEEE ICASSP*, May 2013, pp. 4849–4853.

[125] J. Chen, Y. Hong, and Z. Wang, "Performance of precoding multi-user MIMO indoor visible light communications," in *Proc. IEEE IPC*, 2013, pp. 541–542.

[126] Y. Hong, J. Chen, Z. Wang, and C. Yu, "Performance of a precoding MIMO system for decentralized multiuser indoor visible light communications," *IEEE Photon. J.*, vol. 5, no. 4, Aug. 2013, Art ID. 7800211.

[127] J. Chen, N. Ma, Y. Hong, and C. Yu, "On the performance of MU-MIMO indoor visible light communication system based on THP algorithm," in *Proc. IEEE/CIC ICCC*, Oct. 2014, pp. 136–140.

[128] H. Haas, PureLiFi Attocell. [Online]. Available: www.purelifi.com

[129] Z. Wang, C. Yu, W.-D. Zhong, J. Chen, and W. Chen, "Performance of a novel LED lamp arrangement to reduce SNR fluctuation for multi-user visible light communication systems," *Opt. Exp.*, vol. 20, no. 4, pp. 4564–4573, Feb. 2012.

[130] Z. Wang, W.-D. Zhong, C. Yu, and J. Chen, "A novel LED arrangement to reduce SNR fluctuation for multi-user in visible light communication systems," in *Proc. 8th ICICS*, Dec. 2011, pp. 1–4.

[131] G. Prince and T. Little, "On the performance gains of cooperative transmission concepts in intensity modulated direct detection visible light communication networks," in *Proc. 6th ICWMC*, Sep. 2010, pp. 297–302.

[132] G. Marsh and J. Kahn, "Channel reuse strategies for indoor infrared wireless communications," in *Proc. GLOBECOM, Communications: The Key to Global Prosperity*, Nov. 1996, vol. 3, pp. 1597–1602.

[133] B. Ghimire and H. Haas, "Self-organising interference coordination in optical wireless networks," *EURASIP J. Wireless Commun. Netw.*, vol. 2012, pp. 1–15, 2012.

[134] Q. Wang, D. Giustiniano, and D. Puccinelli, "OpenVLC: Software-defined visible light embedded networks," in *Proc. 1st ACM MobiCom Workshop VLCS*, 2014, pp. 15–20.

[135] BeagleBone Black. [Online]. Available: http://beagleboard.org/

[136] L. P. Klaver, "Design of a network stack for directional visible light communication," Ph.D. dissertation, Faculty Elect. Eng., Math. Comput. Sci., Delft Univ. Technol., Delft, The Netherlands, 2014.

[137] Atmel ATmega328P. [Online]. Available: http://www.atmel.com/tools/mega328p-xmini.aspx

[138] Raspberry Pi. [Online]. Available: https://www.raspberrypi.org/

[139] Arduino. [Online]. Available: https://www.arduino.cc/

[140] WARP project. [Online]. Available: http://warpproject.org

[141] G. Wang, J. Zhang, and X. Zhang, "Dancing with light: Predictive in-frame rate selection for visible light networks," in *Proc. IEEE INFOCOM*, 2015, pp. 2434–2442.

[142] E. Knightly, Y. Qiao, and H. Haas, "A software-defined visible light communications system with WARP," in *Proc. 1st ACM Workshop Visible Light Commun. Syst.*, 2014, pp. 2434–2442.

[143] Q. Wang, D. Giustiniano, and D. Puccinelli, "An open-source research platform for embedded visible light networking," *IEEE Wireless Commun.*, vol. 22, no. 2, pp. 94–100, Apr. 2015.

[144] WikiStart—GNU Radio. [Online]. Available: http://gnuradio.org/redmine/projects/gnuradio/wiki

[145] Universal Softwaere Radio Platform. [Online]. Available: http://www.ettus.com/

[146] M. Rahaim, A. Miravakili, T. Borogovac, T. Little, and V. Joyner, "Demonstration of a software defined visible light communication system," in *Proc. 17th Annu. Int. Conf. Mobicom*, 2011, pp. 1–4.

[147] M. Rahaim *et al.*, "Software defined visible light communication," in *Proc. WInnComm SDR*, 2014, pp. 1–10.

[148] K. Chintalapudi, A. Padmanabha Iyer, and V. N. Padmanabhan, "Indoor localization without the pain," in *Proc. 16th Annu. Int. Conf. MobiCom*, 2010, pp. 173–184.

[149] S. Sen, J. Lee, K.-H. Kim, and P. Congdon, "Avoiding multipath to revive inbuilding WiFi localization," in *Proc. 11th Annu. Int. Conf. MobiSys*, 2013, pp. 249–262.

[150] L. Li, P. Hu, C. Peng, G. Shen, and F. Zhao, "Epsilon: A visible light based positioning system," in *Proc. 11th USENIX Symp. NSDI*. Seattle, WA, USA, Apr. 2014, pp. 331–343.

[151] Y.-S. Kuo, P. Pannuto, K.-J. Hsiao, and P. Dutta, "Luxapose: Indoor positioning with mobile phones and visible light," in *Proc. 20th Annu. Int. Conf. MobiCom*, 2014, pp. 447–458.

[152] N. Rajagopal, P. Lazik, and A. Rowe, "Visual light landmarks for mobile devices," in *Proc. 13th Int. Symp. IPSN*, Piscataway, NJ, USA, 2014, pp. 249–260.

[153] G. Prince and T. Little, "A two phase hybrid RSS/AoA algorithm for indoor device localization using visible light," in *Proc. IEEE GLOBECOM*, Dec. 2012, pp. 3347–3352.
[154] S.-H. Yang, H.-S. Kim, Y.-H. Son, and S.-K. Han, "Three-dimensional visible light indoor localization using AOA and RSS with multiple optical receivers," *J. Lightw. Technol.*, vol. 32, no. 14, pp. 2480–2485, Jul. 2014.
[155] Bytelight—Scalable Indoor Localization with LED. [Online]. Available: www.bytelight.com
[156] A. Ashok *et al.*, "Challenge: Mobile optical networks through visual MIMO," in *Proc. 16th Annu. Int. Conf. MobiCom*, 2010, pp. 105–112.
[157] A. Ashok *et al.*, "Capacity of pervasive camera based communication under perspective distortions," in *Proc. IEEE Int. Conf. PerCom*, Mar. 2014, pp. 112–120.
[158] S. D. Perli, N. Ahmed, and D. Katabi, "PixNet: Interference-free wireless links using LCD-camera pairs," in *Proc. 16th Annu. Int. Conf. MobiCom*, 2010, pp. 137–148.
[159] T. Hao, R. Zhou, and G. Xing, "COBRA: Color barcode streaming for smartphone systems," in *Proc. 10th Int. Conf. MobiSys*, New York, NY, USA, 2012, pp. 85–98.
[160] W. Hu, H. Gu, and Q. Pu, "Lightsync: Unsynchronized visual communication over screen-camera links," in *Proc. 19th Annu. Int. Conf. Mobile Comput. Netw.*, 2013, pp. 15–26.
[161] R. LiKamWa, D. Ramirez, and J. Holloway, "Styrofoam: A tightly packed coding scheme for camera-based visible light communication," in *Proc. 1st ACM MobiCom Workshop Visible Light Commun. Syst.*, 2014, pp. 27–32.
[162] T. Li, C. An, A. T. Campbell, and X. Zhou, "Hilight: Hiding bits in pixel translucency changes," *ACM SIGMOBILE Mobile Comput. Commun. Rev.*, vol. 18, no. 3, pp. 62–70, 2015.
[163] A. Wang *et al.*, "Enhancing reliability to boost the throughput over screen-camera links," in *Proc. 20th Annu. Int. Conf. MobiCom*, 2014, pp. 41–52.
[164] W. Hu *et al.*, "Strata: Layered coding for scalable visual communication," in *Proc. 20th Annu. Int. Conf. MobiCom*, 2014, pp. 79–90.
[165] B. Zhang, K. Ren, G. Xing, X. Fu, and C. Wang, "SBVLC: Secure barcode-based visible light communication for smartphones," in *Proc. IEEE INFOCOM*, Apr. 2014, pp. 2661–2669.
[166] S. Arai *et al.*, "Experimental on hierarchical transmission scheme for visible light communication using LED traffic light and high-speed camera," in *Proc. IEEE 66th VTC-Fall*, Sep. 2007, pp. 2174–2178.
[167] S. Arai *et al.*, "Multiple LED arrays acquisition for image-sensor-based I2V-VLC using block matching," in *Proc. IEEE 11th CCNC*, Jan. 2014, pp. 605–610.
[168] C. Li and S. Shimamoto, "An open traffic light control model for reducing vehicles CO2 emissions based on ETC vehicles," *IEEE Trans. Veh. Technol.*, vol. 61, no. 1, pp. 97–110, Jan. 2012.
[169] C. B. Liu, B. Sadeghi, and E. W. Knightly, "Enabling Vehicular Visible Light Communication (V2LC) networks," in *Proc. 8th ACM Int. Workshop VANET*, 2011, pp. 41–50.
[170] L.-C. Wu and H.-M. Tsai, "Modeling vehicle-to-vehicle visible light communication link duration with empirical data," in *Proc. IEEE GC Wkshps*, Dec. 2013, pp. 1103–1109.
[171] S.-H. You, S.-H. Chang, H.-M. Lin, and H.-M. Tsai, "Visible light communications for scooter safety," in *Proc. 11th Annu. Int. Conf. MobiSys*, 2013, pp. 509–510.
[172] S.-H. Yu, O. Shih, H.-M. Tsai, N. Wisitpongphan, and R. Roberts, "Smart automotive lighting for vehicle safety," *IEEE Commun. Mag.*, vol. 51, no. 12, pp. 50–59, Dec. 2013.
[173] I. Takai *et al.*, "LED and CMOS image sensor based optical wireless communication system for automotive applications," *IEEE Photon. J.*, vol. 5, no. 5, Oct 2013, Art ID. 6801418.
[174] T. Yamazato *et al.*, "Image-sensor-based visible light communication for automotive applications," *IEEE Commun. Mag.*, vol. 52, no. 7, pp. 88–97, Jul. 2014.
[175] Y. Zeng, P. H. Pathak, C. Xu, and P. Mohapatra, "Your AP knows how you move: Fine-grained device motion recognition through WiFi," in *Proc. 1st ACM Workshop HotWireless*, 2014, pp. 49–54.
[176] B. Kellogg, V. Talla, and S. Gollakota, "Bringing gesture recognition to all devices," in *Proc. 11th USENIX Symp. NSDI*, Seattle, WA, USA, Apr. 2014, pp. 303–316.
[177] J. Wang, D. Vasisht, and D. Katabi, "RF-IDraw: Virtual touch screen in the air using RF signals," in *Proc. ACM Conf. SIGCOMM*, 2014, pp. 235–246.
[178] Microsoft Kinect Sensor. [Online]. Available: http://www.xbox.com/en-US/xbox-one/accessories/kinect-for-xbox-one
[179] S. Gupta, K.-Y. Chen, M. S. Reynolds, and S. N. Patel, "LightWave: Using compact fluorescent lights as sensors," in *Proc. 13th Int. Conf. UbiComp*, 2011, pp. 65–74.
[180] P. Dietz, W. Yerazunis, and D. Leigh, "Very low-cost sensing and communication using bidirectional LEDs," in *Proc. UbiComp*, 2003, vol. 2864, ser. Lecture Notes in Computer Science, A. Dey, A. Schmidt, and J. McCarthy, Eds. Berlin, Germany: Springer-Verlag, pp. 175–191.
[181] D. Schmidt, D. Molyneaux, and X. Cao, "PICOntrol: Using a handheld projector for direct control of physical devices through visible light," in *Proc. 25th Annu. ACM Symp. UIST*, 2012, pp. 379–388.
[182] C. Zhang, J. Tabor, J. Zhang, and X. Zhang, "Extending mobile interaction through near-field visible light sensing," in *Proc. 21st Ann. Int. Conf. MobiCom*, 2015, pp. 345–357.
[183] X. Zhou and A. T. Campbell, "Visible light networking and sensing," in *Proc. 1st ACM Workshop HotWireless*, 2014, pp. 55–60.
[184] T. Li, C. An, Z. Tian, A. T. Campbell, and X. Zhou, "Human sensing using visible light communication," in *Proc. 21st Annu. Int. Conf. MobiCom*, New York, NY, USA, 2015, pp. 331–344.
[185] C. An, T. Li, Z. Tian, A. T. Campbell, and X. Zhou, "Visible light knows who you are," in *Proc. 2nd ACM MobiCom Workshop VLCS*, 2015, pp. 39–44.
[186] H. Ma, L. Lampe, and S. Hranilovic, "Integration of indoor visible light and power line communication systems," in *Proc. 17th IEEE ISPLC*, Mar. 2013, pp. 291–296.
[187] M. Yousuf and M. El-Shafei, "Power line communications: An overview—Part I," in *Proc. 4th Int. Conf. IIT*, Nov 2007, pp. 218–222.
[188] M. Rahaim, A. Vegni, and T. Little, "A hybrid radio frequency and broadcast visible light communication system," in *Proc. IEEE GC Wkshps*, Dec. 2011, pp. 792–796.
[189] S. Shao *et al.*, "An indoor hybrid WiFi-vlc Internet access system," in *Proc. IEEE 11th Int. Conf. MASS*, Oct. 2014, pp. 569–574.
[190] C. Lee, C. Tan, H. Wong, and M. Yahya, "Performance evaluation of hybrid VLC using device cost and power over data throughput criteria," in *Proc. SPIE Opt. Eng.+ Appl.*, 2013, Art ID. 88451A.
[191] K.-D. Langer and J. Grubor, "Recent developments in optical wireless communications using infrared and visible light," in *Proc. 9th ICTON*, Jul. 2007, vol. 3, pp. 146–151.
[192] Y.-S. Kuo, P. Pannuto, and P. Dutta, "System architecture directions for a software-defined lighting infrastructure," in *Proc. 1st ACM MobiCom Workshop VLCS*, 2014, pp. 3–8.
[193] D. O'brien *et al.*, "Visible light communications: Challenges and possibilities," in *proc. IEEE 19th Int. Symp. PIMRC*, 2008, pp. 1–5.
[194] D. O'Brien, "Cooperation in optical wireless communications," in *Cognitive Wireless Networks*, F. Fitzek and M. Katz, Eds. Dordrecht, The Netherlands: Springer-Verlag, 2007, pp. 623–634.
[195] J. Ylitalo, T. Jokikyyny, T. Kauppinen, A. Tuominen, and J. Laine, "Dynamic network interface selection in multihomed mobile hosts," in *Proc. 36th Annu. Hawaii Int. Conf. Syst. Sci.*, Jan. 2003, pp. 10–18.
[196] H. Balakrishnan and V. Padmanabhan, "How network asymmetry affects TCP," *IEEE Commun. Mag.*, vol. 39, no. 4, pp. 60–67, Apr. 2001.
[197] J. Classen, J. Chen, D. Steinmetzer, M. Hollick, and E. Knightly, "The spy next door: Eavesdropping on high throughput visible light communications," in *Proc. 2nd ACM MobiCom Workshop VLCS*, 2015, pp. 9–14.

Parth H. Pathak received the doctoral degree in computer science at North Carolina State University, Raleigh, NC, USA, in 2012. He is a Postdoctoral Scholar in the Computer Science Department at University of California, Davis, CA, USA. His current research interests are in design and development of next-generation wireless networks, network analytics, and mobile computing. In the past, he has worked on cross-layer protocol design and optimization of wireless networks.

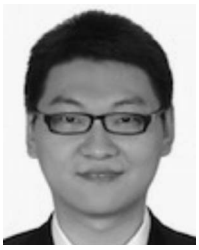

Xiaotao Feng received the B.S. and M.S. degrees in electrical engineering from Beijing Jiaotong University, Beijing, China, in 2009 and Peking University, Beijing, China, in 2012, respectively. He is currently pursuing the Ph.D. degree in the Department of Electrical and Computer Engineering at University of California, Davis, CA, USA. His current research interests include wireless networking, game theory and its applications to the field of multi-agent systems, and cyber security.

Pengfei Hu received the B.S. degree from Changchun University of Science and Technology, Jilin, China, in 2010 and the M.S. from University of Science and Technology of China, Anhui, China, in 2013. He is pursuing the Ph.D. degree in the Department of Computer Science, University of California, Davis, CA, USA. In 2012, he received National Scholarship, which is the top award for graduate students in China. His research interests include mobile computing, visible light communication, and security and privacy.

Prasant Mohapatra received the doctoral degree from Penn State University, State College, PA, USA, in 1993, and received an Outstanding Engineering Alumni Award in 2008. His research interests are in the areas of wireless networks, mobile communications, cybersecurity, and Internet protocols. He is a Professor in the Department of Computer Science and is currently serving as the Associate Chancellor of the University of California, Davis, CA, USA. He was the Department Chair of Computer Science during 2007–2013, and held the Tim Bucher Family Endowed Chair Professorship during that period. He served as the Interim Vice-Provost and the Campus CIO of the University of California, Davis during 2013–2014. In the past, he has been with the faculty of Iowa State University and Michigan State University. He is the Editor-in-Chief of the IEEE TRANSACTIONS ON MOBILE COMPUTING. He has served on the editorial board of the IEEE TRANSACTIONS ON COMPUTERS, IEEE TRANSACTIONS ON MOBILE COMPUTING, IEEE TRANSACTION ON PARALLEL AND DISTRIBUTED SYSTEMS, *Journal of Wireless Networks* (ACM), and *Ad Hoc Networks*. He has served as the Program Chair and the General Chair and has been on the program/organizational committees of several international conferences.